AMERICAN UNIVERSITY OF BEIRUT

SPHINGOLIPIDOMICS OF INFLUENZA A VIRUS-INFECTED LUNG EPITHELIAL CELLS

by
MARIAM IMAD HIJAZI

A thesis
submitted in partial fulfillment of the requirements
for the degree of Master of Science
to the Department of Biochemistry and Molecular Genetics
of the Faculty of Medicine
at the American University of Beirut

Beirut, Lebanon
June 2020

AMERICAN UNIVERSITY OF BEIRUT

Sphingolipidomics of influenza A virus-infected lung epithelial cells

by

MARIAM IMAD HIJAZI

Approved by:

Dr. Ghassan Dbaibo, MD — Advisor
Professor, Biochemistry and Molecular Genetics

Dr. Hassan Zaraket — Co-Advisor
Assistant Professor; Experimental Pathology, Immunology and Microbiology

Dr. Marwan Refaat, MD — Member of Committee
Associate Professor, Biochemistry and Molecular Genetics

Dr. Mazen Kurban, MD — Member of Committee
Associate Professor, Biochemistry and Molecular Genetics

Date of thesis/dissertation defense: [June 19, 2020]

AMERICAN UNIVERSITY OF BEIRUT

THESIS, DISSERTATION, PROJECT RELEASE FORM

Student Name : Hijazi Mariam Imad
Last First Middle

⊗ Master's Thesis ○ Master's Project ○ Doctoral Dissertation

☐ I authorize the American University of Beirut to: (a) reproduce hard or electronic copies of my thesis, dissertation, or project; (b) include such copies in the archives and digital repositories of the University; and (c) make freely available such copies to third parties for research or educational purposes.

☒ I authorize the American University of Beirut, to: (a) reproduce hard or electronic copies of it; (b) include such copies in the archives and digital repositories of the University; and (c) make freely available such copies to third parties for research or educational purposes after:

One ---- year from the date of submission of my thesis, dissertation, or project.

Two ---- years from the date of submission of my thesis, dissertation, or project.

Three ---- years from the date of submission of my thesis, dissertation, or project.

Mariam 6/7/2020

Signature Date

ACKNOWLEDGEMENTS

I would like to express all my respect and gratitude to my advisor Dr. Ghassan Dbaibo for providing me the opportunity to complete my master's project. I truly appreciate his support, encouragement and guidance, his trust in my capacities and his spirit of challenge.

I sincerely thank my co-advisor Dr. Hassan Zaraket for his encouraging guidance and his kind supervision in the achievement of my project.

I would like to thank my committee members, Dr. Marwan Refaat and Dr. Mazen Kurban for reviewing my dissertation and evaluating my work.

My immense appreciation is dedicated to Dr. Lina Reslan for her continuous motivation, her time and her endless help through every step of this work. I would like also to thank her for bestowing her knowledge upon me and incorporating me in diverse experiments in the lab unrelated to my work.

I specially thank Dr. Marguerite Mrad for her continuous support and guidance for the thesis results and discussion.

I also would like to thank Mr. Amer Sakr and Mr. Oussama Yamani from the AUST for the optimization and the performance of the LC/MS experiments.

I would like to take the opportunity to thank Dr. Nadia Soudani for teaching me the procedures and the protocols related to viruses and tirelessly guiding me through the experiments.

I am extremely thankful and pay my gratitude to the CIDR lab members especially the research assistants Marc Finianos and Nancy Hourani for tutoring me, the lab manager Amjad Haidar and my colleague Bahij Moumneh for their continuous help and support.

I would like to acknowledge my parents, my family and my friends for their endless support and for being a constant source of motivation and inspiration during my studies.

Finally, I want to thank GOD for giving me the patience, the persistence and the strength to finish my project.

AN ABSTRACT OF THE THESIS OF

Mariam Imad Hijazi for Master of Science
Major: Biochemistry and Molecular Genetics

Title: Sphingolipidomics of Influenza A virus-infected lung epithelial cells

Introduction: Influenza virus continues to threaten humans and remains a global health concern. Influenza viruses hijack host cell machineries and impact host cell metabolism to tailor cellular pathways and resources to their needs for efficient replication, assembly and budding. Released viruses consist of a host-derived lipid envelope which is a detailed representation of the lipid composition at budding sites. They not only acquire such host lipids, but also have the capacity to actively remodel the lipid host landscape by tuning cellular sphingolipids and regulating different ceramide species. Gaining further insights into how host lipid remodeling occurs upon influenza A virus infection in human lung adenocarcinoma epithelial cell line and how they interfere with ceramide pathways might propose new avenues for development of antiviral molecules and strategies.

Aims: To Establish a detailed lipid profile of infected A549 cell line infected with influenza A virus (IAV) and determine the impact of IAV infection on cellular sphingolipid metabolism.

Methods: A549 were infected with IAV A/Puerto Rico/8/34 (PR8) at 1pfu/cell, and then harvested at different time points starting 15 minutes to 48 hours post-infection (hpi). Lipids were extracted and characterized using liquid chromatography-mass spectrometry (LC/MS/MS). Quantitative real-time PCR was performed to assess the expression levels of many key enzymes involved in the sphingolipid metabolic pathways.

Results: IAV infection induced changes in host cell lipid metabolism leading to an increase in ceramide species in a time dependent manner marking the highest increase at 48 hpi compared to non-infected controls. IAV also induced an increase in lactosylceramide at later time points (36 and 48 hpi). Moreover, some sphingomyelin species were downregulated upon infection compared to non-infected cells at 36 hpi.

Conclusion: IAV induces modifications in the A549 sphingolipidome. Ceramide exerts an antiviral role by inducing an accumulation at late time points.

CONTENTS

ILLUSTRATIONS

ABBREVIATIONS

ASMase: Acid sphingomyelinase

BSA: Bovine serum albumin

C1P: Ceramide-1-phosphate

CERT: Ceramide transfer proteins

CerS: Ceramide synthase

cRNA: Complimentary RNA

DES: Dihydroceramide desaturase

ER: Endoplasmic reticulum

FBS: Fetal bovine serum

HA: Hemagglutinin

hpi: Hours post-infection

HPLC: High performance liquid chromatography

IAV: Influenza A virus

LC/MS: Liquid chromatography / Mass spectrometry

M1: Matrix 1

M2: Matrix 2

MDCK: Madin-Darby canine kidney

MEM: Minimal essential media

mRNA: Messenger RNA

MOI: Multiplicity of infection

NA: Neuraminidase

NEP: Nuclear export protein

NLSs: Nuclear localization signals

NP: Nucleoprotein

NPC: Nuclear pore complex

NSMase: Neutral sphingomyelinase

NSP1: Non-structural protein 1

NSP2: Non-structural protein 2

PA: Polymerase acidic protein

PB1: Polymerase basic protein 1

PB2: Polymerase basic protein 2

PB1-F2: Polymerase basic protein 1 F2

PBS: Phosphate buffer saline

S1P: Sphingosine-1-phosphate

SM: Sphingomyelin

SK: Sphingosine kinase

SK1: Sphingosine kinase 1

SK2: Sphingosine kinase 2

SPT: Serine palmitoyltransferase

vRNA: Viral RNA

vRNP: Viral Ribonucleoprotein

CHAPTER I

INTRODUCTION

A. Influenza virus

Influenza, an acute respiratory illness caused by influenza virus, remains a major worldwide health concern [1]. Influenza viruses, members of *Orthomyxoviridae* family, can infect a variety of mammalian and avian species including humans [2, 3] (Figure 1). They are classified as either types A, B, C, or the recently identified type D. Influenza A and B viruses cause seasonal epidemics, whereas influenza C virus infection are rare [4]. The natural reservoir for type A is wild aquatic birds and humans while the only natural reservoir for type B is human being [5, 6].

Influenza can spread rapidly through communities infecting epithelial cells of the upper and lower respiratory system, causing symptoms of fever and cough [7, 8]. Every year, seasonal influenza virus epidemics result in approximately three to five million cases of severe illness and in 290,000 to 650,000 deaths worldwide [9].

1. Influenza A virus

Influenza A virus (IAV) is the major etiologic agent of acute respiratory tract infections. It is the most common and virulent pathogen among the other types of influenza [10]. It is divided into subtypes based on the serological reactivity to the combination of surface glycoproteins, the hemagglutinin (HA) and the neuraminidase (NA) [11]. The antigenic variation in the HA is caused by two mechanisms known as antigenic drift and

antigenic shift. The antigenic drift is regulated by a variety of mutations in the HA genes due to the viral RNA polymerase that lacks proofreading activity when transcribing the influenza genome. The antigenic shift refers to the transmission of an animal or avian virus from an animal reservoir to humans or to the reassortment of the HA gene segment between animal and human influenza A viruses [12-14].

Out of 16 HA (H1-16) and 9 NA subtypes (N1-9) found in IAVs isolated from aquatic birds [15], three were associated with pandemics in 1918 and 2009 by H1N1, in 1957 by H2N2, and in 1968 by H3N2 [9, 16].

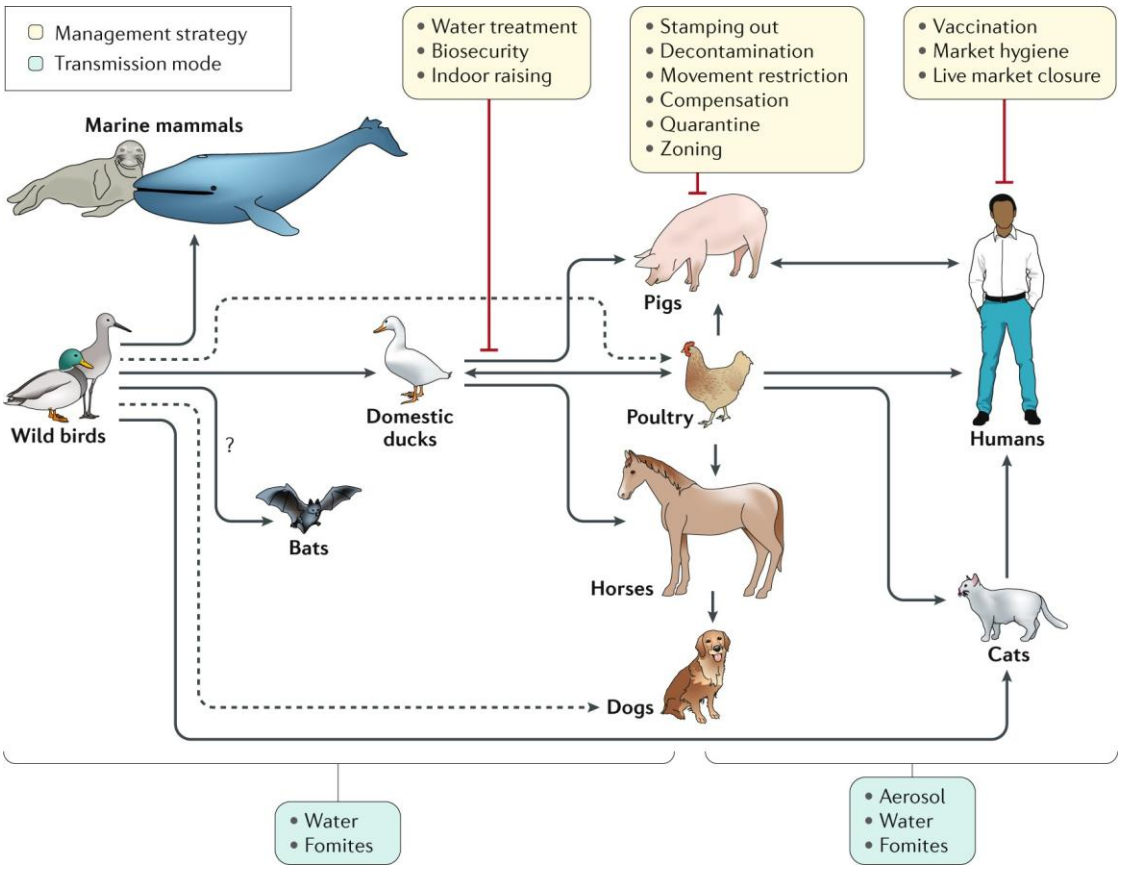

Figure 1. Schematic representation of IAV reservoir and transmission mode

Influenza viruses from wild birds can spill over through water or fomites to marine mammals and to domestic free-range ducks with the possible infection of bat with influenza-like virus. Transmissions to other avian species from domestic ducks or directly from wild birds can also occur from contaminated water. Transmission from ducks to other species occurs through 'backyard' farming, where animals are raised together. Humans can be infected with poultry and swine influenza viruses through aerosols, fomites or contaminated water. Human-to-human transmission of seasonal or pandemic human viruses can be mediated by respiratory droplets, aerosols or self-inoculation from fomites. Other domestic animals known to be susceptible to influenza virus infections are dogs and cats. Dashed lines represent transmission that bypasses a domestic duck intermediate. Adapted from *Influenza* by Krammer *et al.* (2018) [17]

a. Influenza A virus structure

IAV is an enveloped virus that contains eight negative senses, single-stranded viral RNA gene. These segments are numbered in order of decreasing length and found as individual viral ribonucleoprotein (vRNP). Each vRNP is wrapped around numerous copies of nucleoprotein and bound by a single copy of the polymerase acidic protein (PA) and the polymerase basic proteins (PB1, PB2 and PB1-F2) [13, 18, 19]. They encode essential viral protein including the viral transmembrane HA, NA, matrix 1 (M1), matrix 2 (M2), the nucleoprotein (NP), and the non-structural proteins (NSP1 and NSP2) [20, 21] (Figure 2).

Morphologically, IAVs can either form spheres with a diameter of ~100 nm or filaments that can reach up to 20 μm in length [22, 23]. The viral particle is composed of a phospholipid bilayer membrane derived from the host plasma membrane [24, 25].

HA and NA mediate viral entry and release respectively into a host [26, 27]. M1 maintains the integrity and shape of the intact viral particle [28, 29], whereas M2 is a proton-selective ion channel involved in virus assembly and budding, as well as virus uncoating during the entry into host cells [22, 30]. NS1 plays a critical role in evasion of

host immunity [31] and NS2 facilitates the export of newly synthesized vRNPs from the nucleus to the cytoplasm for packaging [32].

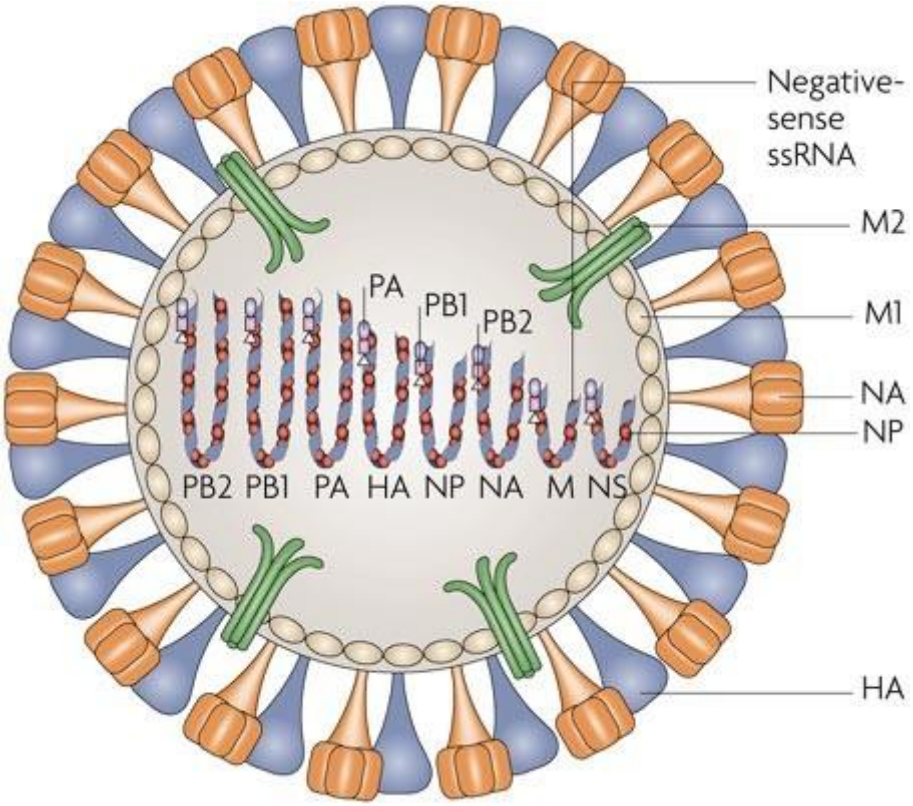

Figure 2. Schematic diagram of IAV

Three viral proteins (HA, NA and M2) are inserted through the lipid bilayer of the viral membrane. The matrix protein M1 underlies the lipid bilayer and interacts with ribonucleoprotein complexes. Within the envelope, there are eight segments of single strand RNA genome in the form of RNP forming a complex of three polymerase proteins (PB2, PB1 and PA), NP and RNA. Adapted from *The evolution of epidemic influenza* by Nelson *et al.* (2007) [33]

b. Influenza A life cycle

i. Entry into the host cell

The life cycle of IAV is initiated by the binding of influenza virus particles to the host cell surface. The attachment into the host cells requires interactions between the viral HA, concentrated in microdomains on the viral envelope, and sialic acid residues present on the cell surface [34]. The HA precursor, HA0, is made up of HA1 containing the receptor binding domain, and HA2 that contains the fusion peptide, linked by disulphide bonds [35, 36]. Viruses from humans recognize the α (2, 6) linkage, whereas those from avians recognize the α (2, 3) linkages [37].

Upon binding to the host cell's sialic acid residues, receptor-mediated endocytosis occurs and the virus is trafficked to the endosome [38]. The endocytosis can either occur in a clathrin-dependent manner, involving dynamin and the adaptor protein Epsin-1, or by macropinocytosis [22, 39]. The endosome has a low pH of around 5 to 6, which induces a conformational change in cleaved HA molecule, exposing the HA2 fusion peptide [35] and activating the M2 ion channel. Opening M2, the proton-selective ion channel acidifies the viral core. This acidic environment in the virion releases the vRNP from M1 enabling the transfer of the vRNPs to the host cytoplasm [40, 41].

ii. Entry of vRNPs into the nucleus

Transport of released vRNPs into the nucleus via the nuclear pore complex (NPC) is mediated by NP carrying three nuclear localization signals (NLSs) [42].

The viral proteins that make up the vRNP are NP, PA, PB1, and PB2. All of these proteins have known NLSs that can bind to the cellular nuclear import machinery and, thus, enter

the nucleus. Although it is unclear which NLS is crucial for vRNP nuclear entry, it is known that the import occurs via the Crm1 dependent pathway by binding to various karyopherins like importin α and β [42, 43].

ii. Influenza virus replication

The replication of the influenza genome involves the transcription of complimentary RNA (cRNA) followed by the transcription of new viral RNA (vRNA) copies using the cRNAs as templates [44-46]. The cRNAs are produced by an unprimed process that uses the 3′ end of the vRNA template. They are then associated with newly synthesized NP molecules and a single copy of the viral polymerase to form a cRNP. The newly produced viral polymerases incorporated into the cRNPs generate the vRNA copies [47].

In the nucleus, vRNA is transcribed into positive sense RNA species by the vRNA dependent RNA polymerase [41]. The polymerase is a heterotrimer composed of subunits PA, PB1 and PB2. Transcription of viral mRNA from the vRNA templates occurs through a mechanism termed cap snatching in which the viral polymerase uses the PB2 subunit to bind to 5′ caps of short oligomers derived from host pre-mRNA, the PA subunit endonuclease domain to cleave nucleotides downstream of the 5′ cap and the PB1 subunit as mRNA synthesis primer [45, 48]. Each transcript is polyadenylated through a stuttering process when the polymerase encounters the short poly-U sequence at the vRNA 5′ end [49].

The newly synthesized vRNAs are packaged into RNPs and exported into the cytoplasm. The export mechanism is regulated by interactions of viral proteins NEP/NS2 and M1 with the nuclear pore complex [34].

Virus replication within a host cell is a complex interplay of host and viral factors that requires interference and inhibition of antiviral responses. NS1 is highly expressed in infected cells but not incorporated into infectious influenza virions. It is a multifunctional protein localized to the nucleus and cytoplasm consisting of a N-terminal RNA binding domain and a C-terminal "effector" domain which mediates both, binding to host proteins and stabilizing the RNA binding domain. Along with antagonizing interferon-α/ß mediated antiviral responses, NS1 also executes multiple functions to ensure proper virus replication including regulation of vRNA synthesis, mRNA splicing and translation, virus particle morphogenesis, suppression of apoptosis through activation of PI3K/Akt signaling and enhancement of virus pathogenesis [31, 50-53].

Following nuclear export, the translation of the viral mRNAs is divided between cytosolic ribosomes for PB1, PB2, PA, NP, NS1, NS2, and M1 and endoplasmic reticulum (ER)-associated ribosomes for the membrane proteins HA, NA, and M2. At this point, the vRNPs are trafficked toward the plasma membrane for viral assembly by Rab11 [54, 55]. Rab11 transport vesicles emerge from endocytic recycling compartments, specific organelles close to the nucleus composed of tubular organelles [56].

iv. Virus Assembly and budding

Influenza virus acquires it envelope by budding through the plasma membrane. Since virus particles bud from the apical side of polarized cells, HA, NA, and M2 are transported to the apical plasma membrane [57]. M2 plays an important role in the formation of viral particles [30] and M1, present underneath the lipid bilayer, binds lipids, vRNPs as well as the tails of HA and NA [28]. NA on its turn removes the sialic acid

residue from the glycoproteins and glycolipids so the viral particle can be released from the plasma membrane [58].

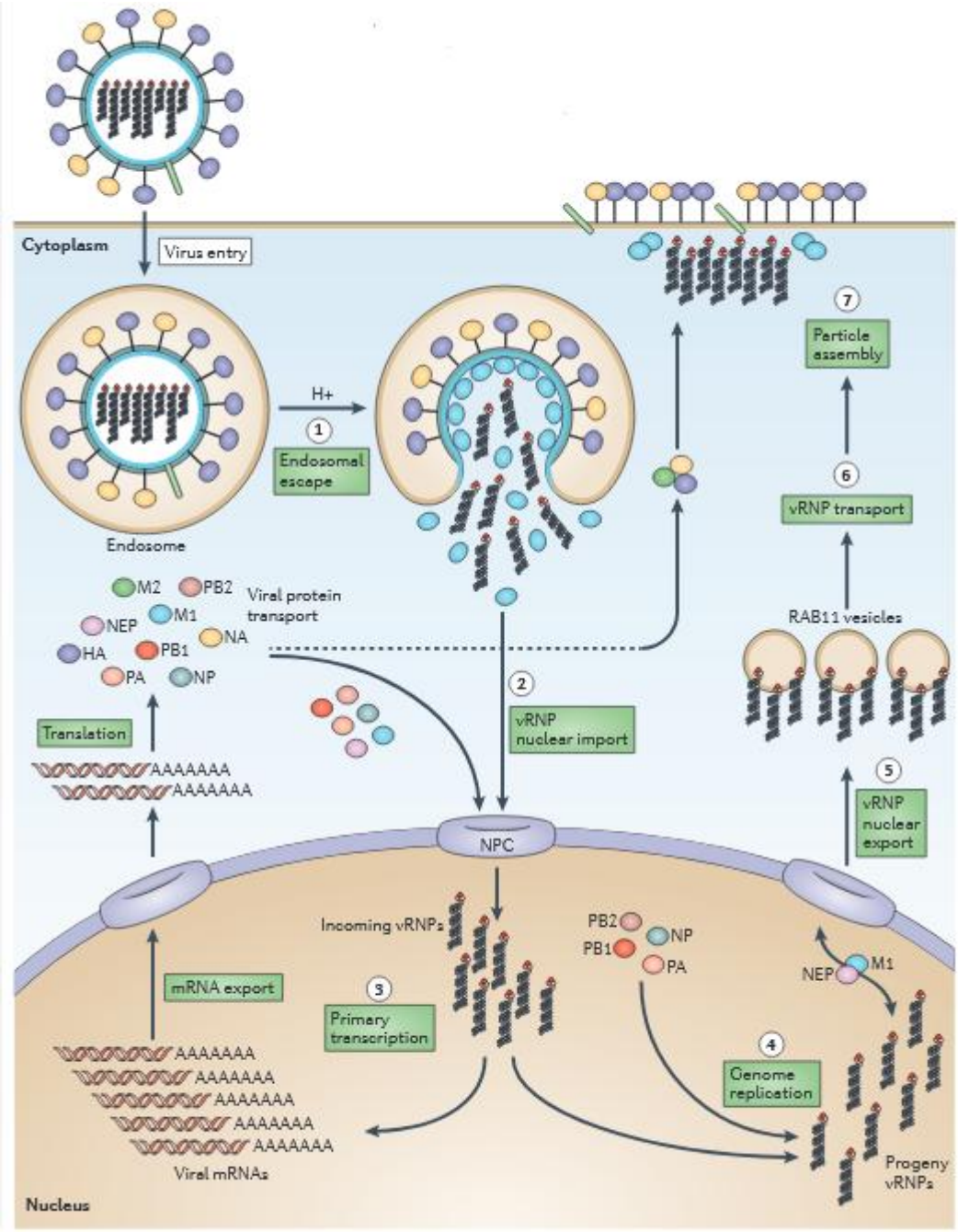

Figure 3. Schematic representation of IAV life cycle

IAV enter cells by endocytosis after the HA binding to host receptor molecules at the plasma membrane. Following internalization, endosomal acidification activates conformational changes in HA, which leads to fusion between the virion and endosomal membranes, providing the vRNPs an access to the cytoplasm (step 1). The viral M2 ion channel promotes acidification of the virion interior, which dissociates the M1 matrix protein from the viral genome. vRNPs that are released from endosomes are transported into the nucleus through the NPC (step 2). Primary transcription results in the production of viral mRNAs are exported to the cytoplasm and translated into proteins by cellular ribosomes (step 3). Newly translated viral proteins are transported to the nucleus (PB1, PB2, PA, nucleoprotein (NP), M1 and nuclear export protein (NEP)) or the plasma membrane (HA, neuraminidase (NA) and M2). After translation and nuclear entry of PB1, PB2, PA and NP, genome replication ensues (step 4). Progeny vRNPs are then exported to the cytoplasm with the assistance of the M1 and NEP proteins (step 5). Newly exported vRNPs are subsequently trafficked to the plasma membrane on RAB11 vesicles (step 6). vRNPs are then incorporated into progeny virus particles containing HA, NA, M2 and M1 (step 7). Finally, virus release from the plasma membrane is mediated by the activities of M2 and NA. Adapted from *At the centre: influenza A virus ribonucleoproteins* by Eisfeld *et al.* (2015) [59]

c. Influenza A virus antivirals

Influenza virus infection can be treated with three classes of antiviral drugs: M2 ion channel inhibitors such as amantadine and rimantadine, NA inhibitors including oseltamivir, zanamivir, peramivir, and laninamivir [60, 61], and a selective inhibitor of influenza cap-dependent endonuclease such as baloxavir marboxil [62]. Amantadine and rimantadine inhibit virus replication by blocking the M2 ion channel on its transmembrane domain, whereas NA inhibitors disrupt the release of progeny virions [63-65]. Baloxavir marboxil is unique in that it inhibits viral replication by targeting the endonuclease function encoded by the PA subunit of the viral polymerase complex [62]. Unfortunately, these drugs are being associated with rapid emergence of drug-resistant strains. Drug resistance refers to reduction in the effectiveness of a drug incurring a disease and it occurs when the microorganism changes its genetic material [66].

Human IAVs viruses have a propensity for the rapid emergence of resistance following antiviral therapy due to their heterogeneous genetic background [67, 68] . For example the oseltamivir-resistance can be conferred by a point mutation in the virus neuraminidase gene resulting in substitution of histidine by a tyrosine at the position 275 of the N1 neuraminidase referred as H274Y mutation [69, 70]. The oseltamivir-resistant H1N1 virus emerged first in North Europe in 2007 and then it spread worldwide in 2008 and 2009 [71].

Adamantane-resistant were also reported during the 1980 epidemic among the seasonal H1N1 and H3N2 subtypes and during 2005-2006 influenza season, where 15.6% of the H1N1 and 90.6% of the H3N2 global isolates were reported adamantane-resistant. This emerging resistance led the Centers for Disease Control and Prevention (CDC), USA, to issue an advisory against the use of this drug as a treatment for IAV infections [72]. The virus ability to develop resistance that reduces the efficacy of the drugs highlights the urgent need for new therapeutic targets that are not influenced by IAV genetic diversity [67]. Some novel findings propose new avenues for development of antiviral molecules and strategies against influenza based on sphingolipids metabolism and ceramide analogues [10].

B. Sphingolipids

Sphingolipids are a complex group of lipids that are found in a wide variety of prokaryotic and eukaryotic organisms as well as viruses [73]. In eukaryotic cells, sphingolipids constitute an important component of cellular membranes; they maintain the integrity of their structure and organization [74]. Their metabolites play numerous roles in cellular biology, including apoptosis, cell-cycle arrest, differentiation, migration, proliferation, and senescence [75].

Most sphingolipids can be metabolized via the activity of multiple enzymes localized in specific sub-cellular compartments [76]. The regulation of the enzymes such as sphingomyelinases, ceramidases, ceramide synthases and cerebrosidases can create discrete cellular pools of sphingolipids, thereby complicating the evaluation of sphingolipid metabolism [77]. These sphingolipid-mediated biologies have been implicated in metabolism, neurodevelopment, inflammation, cancer, and several other physiological and pathological processes [78].

1. Sphingolipids Structure and Nomenclature

Sphingolipids are amphiphilic lipids consisted of a ceramide backbone attached to highly diverse sugar head groups [79]. The ceramide backbone can either be a dihydroceramide in which a sphinganine (saturated sphingoid base) is attached to a fatty acid or a ceramide consisted of a sphingosine (unsaturated sphingoid base) attached to a fatty acid [80] (Figure 4).

To distinguish sphingolipids species, International Union of Pure and Applied Chemistry adopted a nomenclature system that relies on the abbreviation d18:1 in which the first number represents the number of carbon atoms and the second number indicate the number of double bonds. The letter‘d’ refers to the 2 (di-) hydroxyl groups. For example d18:1/14:0 represents a sphingolipid having 2 hydroxyl groups and an 18 carbon chain with a double bond attached to a saturated 14 carbon N-acyl derivative.

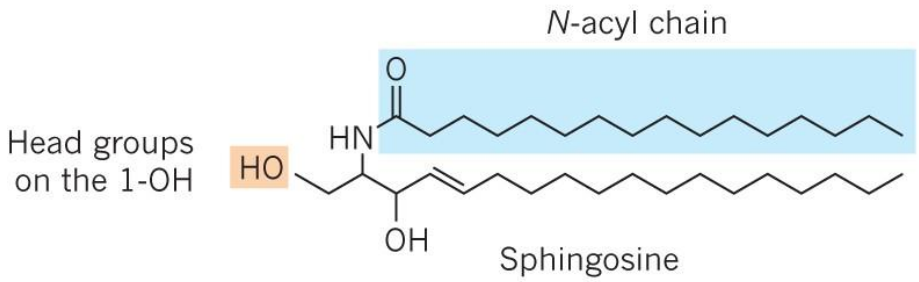

Figure 4. Sphingosine structure

Adapted from *Sphingolipid metabolites in inflammatory disease* by Maceyka *et al.* (2014) [81]

2. Ceramide

Ceramide is a central molecule of sphingolipid metabolism that was first discovered as a structural component of cellular membranes and then emerged as a bioactive lipid [82]. This class of sphingolipids acts a as second messenger molecule that mediate multiple cellular functions such as stress response, apoptosis and growth arrest. They also maintain membrane dynamics, fluidity, and internal membrane transport [83-88].

Ceramide serves also as a metabolic and structural precursor for complex sphingolipids, which are composed of hydrophilic head groups, such as sphingomyelin (SM), ceramide-1-phosphate (C1P) and glucosylceramide [89-91].

Natural ceramides are composed of a sphingosine base and amide-linked acyl chains [92] varying in length from C14 to C26 [87], saturation and hydroxylation [93] (Figure 5). They are highly hydrophobic and insoluble in water [94] and their metabolism comprises at least 28 enzymes that generate over 200 structurally distinct ceramide specie [95].

Ceramide is produced through three distinct metabolic pathways: *de novo* biosynthesis, SM hydrolysis, and salvage pathway [96].

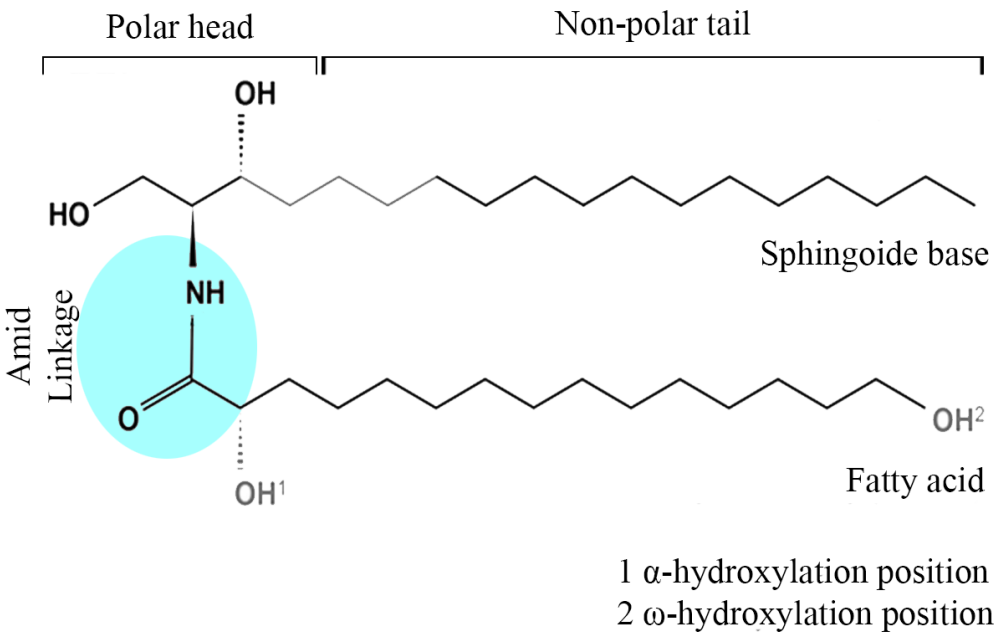

Figure 5. Schematic representation of basic chemical structure of ceramides

Sphingoid base attached to a fatty acid by an amide linkage. The sphingoid base contains a polar head group and a non-polar tail group and the fatty acid contains positions for α- and ω-hydroxylation.

a. *De novo* pathway

De novo biosynthesis of ceramides begins in the lumen of ER and ER-associated membranes [97]. The synthesis starts with the condensation of serine and palmitoyl coenzymeA, a rate-limiting step catalyzed by serine palmitoyltransferase (SPT), to produce 3-keto-dihydrosphingosine (3-Ketosphinganine) [98, 99]. 3-Ketosphinganine is then reduced by reductase and NADPH+H to sphinganine (dihydrosphingosine) [100], which is later acylated by ceramide synthase (CerS) to form dihydroceramide [101]. Six different CerS can be co-expressed in different tissues displaying a high selectivity for acylCoA of different lengths and regulating the biosynthesis of molecular species of ceramides [102, 103]. The last step of de novo sphingolipid synthesis is catalyzed by dihydroceramide desaturase (DES) [104], which inserts a double bond between carbons 4 and 5 of the sphingoid backbone to produce ceramide [100, 105] (Figure 6). Finally, ceramide is transported to the Golgi either via ceramide transfer proteins (CERT) or vesicular trafficking to be further metabolized into more complex sphingolipids ceramides [106, 107].

This pathway can be metabolically induced in response to chemotherapeutic agents [108], heat stress [109], oxidized LDL [110], and cannabinoids [111].

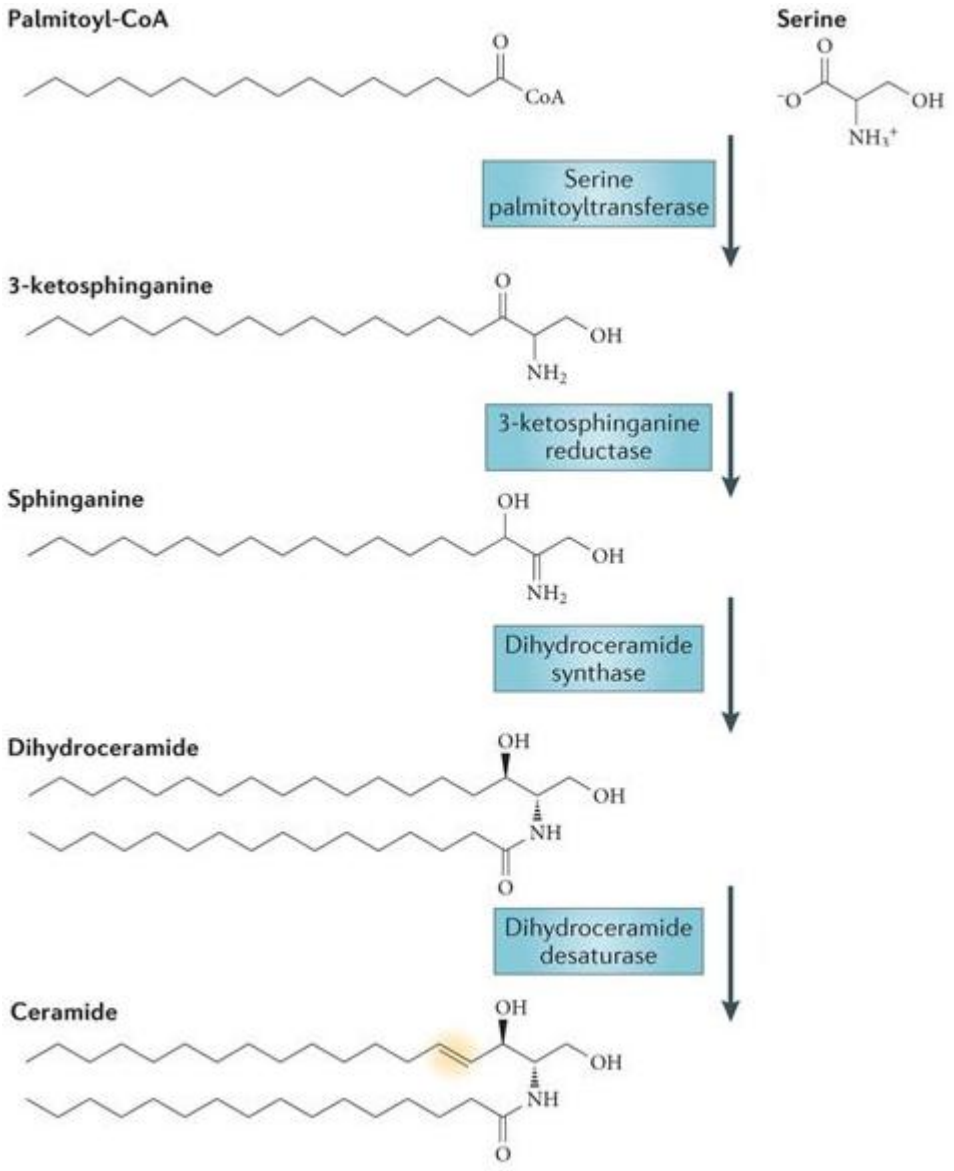

Figure 6. Schematic presentation of the *de novo* pathway.

Adapted from *Potentiation of cannabinoid-induced cytotoxicity in mantle cell lymphoma through modulation of ceramide metabolism* by Gutafsson *et al.* (2009) [112]

b. SM Hydrolysis

The hydrolysis of SM, the most abundant membrane sphingolipid, also generates ceramide. This process is catalyzed mainly by acid or neutral sphingomyelinase (SMase) within the plasma membrane or lysosomes [113]. SM has a long-chain sphingosine base with anamide-linked fatty acyl chain and a phosphorylcholine headgroup at the (1) position of the hydrocarbon backbone. This sphingolipid is associated with cell growth, differentiation, and apoptosis.

SM hydrolysis is activated in response to anticancer drugs, oxidants, and other cellular stresses [114].

c. Salvage Pathway

In the salvage pathway, complex sphingolipids such as glucosylceramide, the precursor for glycolipids like lactosylceramide and gangliosides [115], are degraded into sphingosine and free fatty acid by ceramidases [116]. Ceramide is then produced from the recycled sphingosine through reacylation [82].

This recycling pathway involves a number of key enzymes including glucocerebrosidase (acid-β-glucosidase), ceramidases, and dihydroceramide synthases [117].

d. Ceramide Catabolism

Ceramide is phosphorylated by sphingosine kinases (SK) to form sphingosine-1-phosphate (S1P) [118], which has potent bioactivities generally opposite to those of ceramide [10]. Two distinct SK isoforms, SK1 and SK2, were detected in mammals. SK1 is stimulated by growth and survival factors, generating S1P implicated in the irmitogenic and

anti-apoptotic effects. In contrast to SK1, overexpression of SK2 suppresses growth and enhances apoptosis, suggesting that their different subcellular localizations might be affecting their physiological functions [119].

S1P can be deactivated by S1P phosphatase or broken down by S1P lyase to ethanolamine-1-phosphate [120]. The S1P degradation is irreversible, thus maintaining the balance between ceramide and S1P is crucial for cells, as these bioactive lipids substantially contribute to cell fate decisions [121].

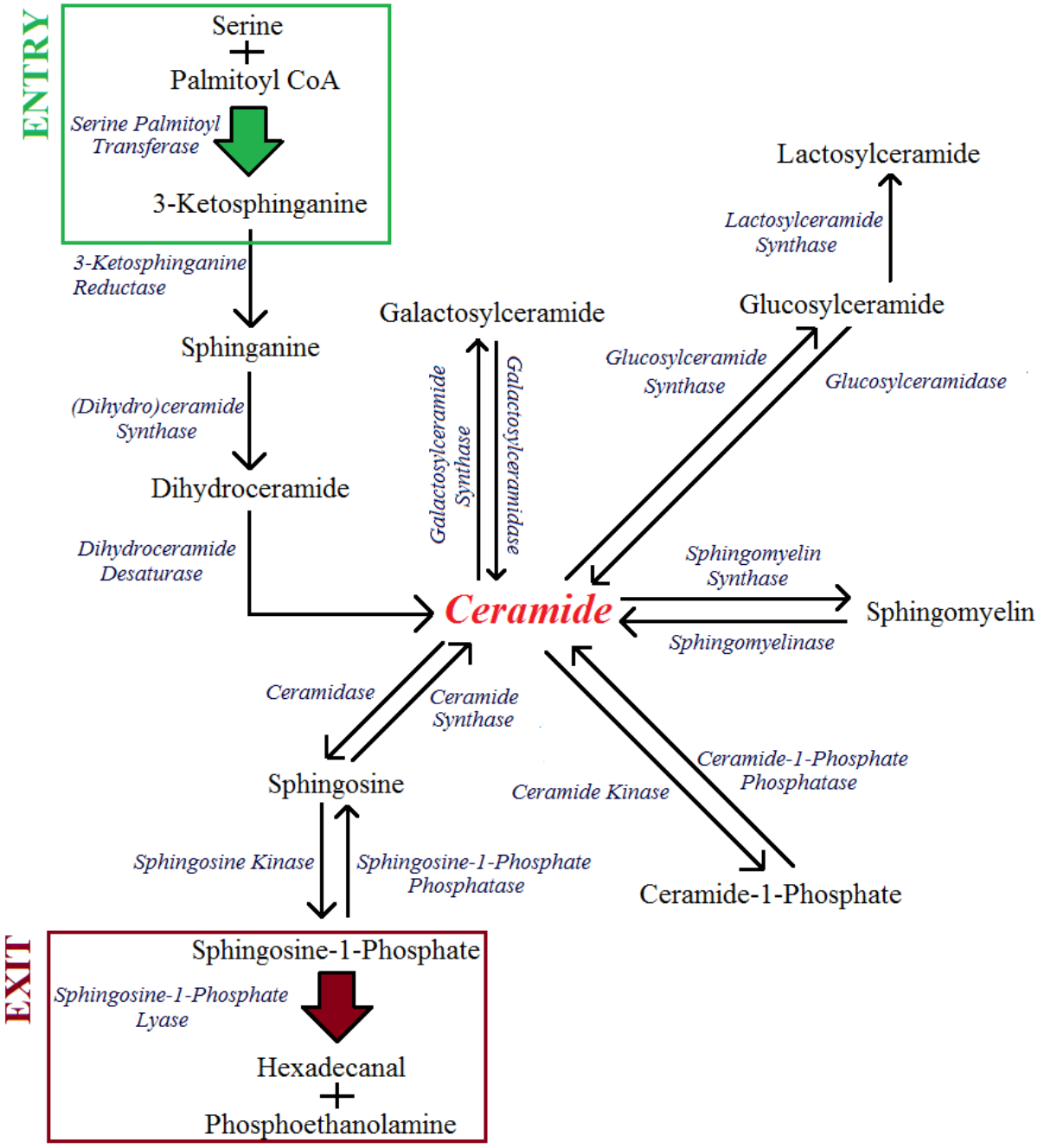

Figure 7. The scheme shows metabolic pathways for ceramide synthesis composed of the sphingomyelinase pathway, the de novo pathway and the salvage pathway.

C. Role of sphingolipids in the influenza virus life cycle

Sphingolipids were shown to play different important roles in virus-host interactions and found to be critical to all stages of the virus life cycle as they are capable of promoting virus binding, entry, replication and even new particle release [38, 122]. Since sphingolipids are modulators of biophysical membrane properties such as fluidity and polarity [123, 124] and regulate membrane deformation, vesiculation, and signal transduction [125, 126], viruses tend to encode proteins that co-opt lipid signaling and synthesis machinery responsible of remodeling the host cell. This action not only generates lipids for envelopment but also establish protected sites of replication [127].

1. Role of sphingolipids during influenza virus entry

The attachment and entry of the viral particle into the host cell requires interactions between the viral HA, concentrated in microdomains enriched with cholesterol and various sphingolipids such as SM and glycosphingolipids, and sialic acid residues present on the cell surface. This interaction leads to the formation of the virus's envelope, derived from the host cell's plasma membrane and consisting of a lipid bilayer involving almost all sphingolipid classes [24].

Upon binding to the host cell, virus entry is mediated by endocytosis, which is regulated by glucosylceramidase, the enzyme that degrades the glucosylceramide to produce a ceramide. Recent studies showed that glucosylceramidase is necessary for influenza virus particles to fuse in endosomes. Glucosylceramidase deficiency diminished the entry and infection of influenza A virus and inhibited the degradation of critical growth factor receptors required

for proper growth control due to a defect in trafficking viral particles into the endosomes [38].

2. Role of sphingolipids during influenza virus replication

The enzyme SK1, which converts sphingosine into S1P, is seen to be increased during virus replication suggesting that S1P might be increasing to favor virus replication. On the other hand, S1P lyase overexpression, which irreversibly degrades S1P, inhibited the expression of influenza virus proteins and the production of infectious progeny viruses. Therefore, S1P lyase expression or activation might suppress influenza virus replication (Figure 8). The mechanism that associates the S1P lyase levels to the influenza virus replication is still unknown; it is suggested to be involved in the activation of ERK and JAK/STAT signaling pathways, since S1P lyase overexpression induces the activation of ERK, and STAT1/STAT2 upon influenza virus infection [1, 128].

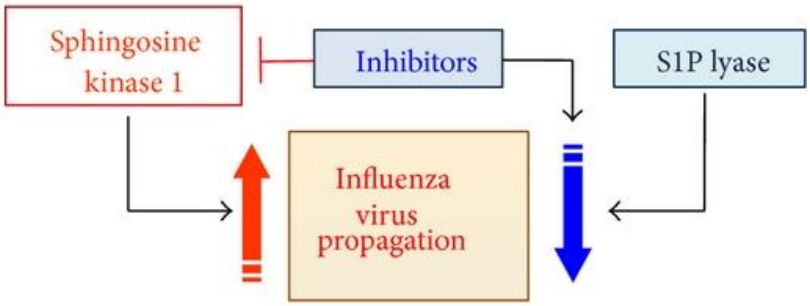

Figure 8. Modulation of influenza virus amplification by sphingosine kinase 1 and S1P lyase.

SK1 increases influenza virus replication, whereas S1P lyase inhibits virus propagation. Manipulation of SK1 such as SK1 inhibition suppresses production of infectious influenza viruses. Adapted from *Transient inhibition of sphingosine kinases confers protection to influenza A virus infected mice* by Xia *et al.* (2018) [129].

3. Role of sphingolipids in influenza virus assembly and budding

Influenza uses lipid rafts microdomains on the cell surface as platforms for viral assembly. Newly synthesized HA and NA concentrate in microdomains enriched for SM and cholesterol [56]. SMase deficient cells reduced transport of the influenza virus HA and NA to the cell surface, where viral maturation, budding, and release occur. This suggests that SM biosynthesis pathway is essential for intracellular transport of influenza A virus glycoproteins and host SM might be responsible for targeting the HA and NA to the cell membrane [130].

CHAPTER II

THESIS OBJECTIVES AND AIMS

The role of sphingolipids in the response to IAV infection is the subject of an ongoing collaboration between the laboratories of Drs. Zaraket and Dbaibo. Previous work demonstrated that ceramide exerts an antiviral role during IAV replication. The ceramide levels significantly increased in a time dependent manner starting 24 h post-infection (hpi) and continued to rise until 48 hpi. The ceramide was shown to be synthesized through *de novo* pathway as its inhibitors Myriocin and Fumonisin B1 abrogated the mentioned accumulation. The inhibition of the *de novo* ceramide pathway was also associated with a significant increase in total viral RNA and a slight increase in viral progeny revealing that IAV replication and production was enhanced upon blocking this biosynthetic pathway. On the other hand, treatment of A549 cells with exogenous C6-ceramide, a synthetic cell-permeable ceramide analogue, followed by IAV infection suppressed virus replication, reduced virus titers and promoted cellular ceramide levels [10].

Another study showed that SM depletion of the plasma membrane or the viral envelope impaired IAV attachment and internalization demonstrating that IAV required SM in both cell membrane and viral envelope for efficient virus entry. SM in the host cells promoted IAV replication. Moreover, ASMase activity was found not to be essential for IAV infection as treating with desipramine, a functional inhibitor of ASMase, did not affect IAV yield. On the contrary, cells infected with IAV showed a significant decrease in ASMase activity at 6, 24, and 48 hpi, with a low residual enzymatic activity at 48 hpi; this

might indicate that IAV possibly inhibits ASMase activity at later stages of infection to preserve SM for subsequent infection cycles [131].

This ceramide accumulation triggered by IAV and the SM requirement for an efficient virus entry prompted us to investigate the regulation of sphingolipids to better understand their role during IAV infection. We decided to utilize a sphingolipidomic approach using the highly sensitive LC-MS technology in order to establish a detailed lipid profile of infected human lung epithelial cell line A549 with IAV and determine the impact of infection on cellular sphingolipid metabolism. This method will also assess the regulation of cellular ceramide levels and determine which ceramide species are modulated in response to IAV infection; thus identify the major sphingolipid pathways that regulate ceramide synthesis during IAV. Additionally, we applied real-time gene expression analysis of sphingolipid enzyme genes in order to quantify the expression levels of different key enzymes involved in ceramide metabolism in response to IAV infection.

CHAPTER III

MATERIALS & METHODS

A. Cell line

Madin-Darby canine kidney (MDCK, ATCC) and human lung adenocarcinoma epithelial cell line (A549, ATCC) were cultured in Dulbecco modified Eagle medium-high glucose (sigma), supplemented with 10% fetal bovine serum (FBS) and 1% of 100 units/ml penicillin-streptomycin (Gibco) and maintained in humidified incubator at 37°C with 5% CO2.

B. Virus propagation and titration

For virus propagation, MDCK cells were infected by influenza Virus A/Puerto Rico/8/34 (PR8) prepared in VIM composed of minimal essential media (MEM) supplemented with bovine serum albumin (BSA; 0.3%), penicillin-streptomycin (5%), MEM vitamin (5%), glutamine (2 mM), and gentamicin (0.04 mg/ml).

Infection was done using a multiplicity of infection (MOI) equivalent to 0.01 PFU/cell. The cells were incubated for one hour to allow adsorption by a gentle shaking every 15 minutes. The infected cells were incubated in VIM containing 1 ug/ml TPCK-trypsin (sigma) for 48 to 72 hpi. After observing the cytopathic effect, the supernatant containing the virus was collected and stored at –80°C.

Virus titration was performed using a plaque assay. Briefly, MDCK cells were seeded at a density of 700,000 cells/well in six-well plates to form a homogeneously confluent monolayer. The cells were then washed with phosphate buffer saline (PBS) supplemented

with calcium and magnesium. 10-fold serial dilutions of the virus were prepared. A volume of 200 µL of virus dilutions was added to each well for 1 hour with a gentle shaking every 15 minutes. Afterwards, the cells were covered with 3 ml of freshly prepared agarose (0.5%) nutritive overlay and kept at room temperature for 10 min to allow their solidification, then incubated at 37°C. After 72 hours, the overlay agarose was removed, and the cells were fixed and stained with crystal violet solution. Plaques, which correspond to dead cells unstained by the dye, were counted until no additional plaques were observed.

C. Virus infection

A549 cells were seeded at a density of 1,000,000 cells/well in a six-well plate and incubated for 24 hours. Cells were washed with PBS supplemented with calcium and magnesium twice then infected with influenza virus A/Puerto Rico/8/34 (PR8) at a MOI of 1 PFU/cells. Plates were gently swirled every 15 minutes for 1 hour in order to ensure complete coverage of cells. Subsequently, virus supernatants and cell lysates were collected at 15 minutes and 30 minutes after infection. For the other time points, one hpi, the virus was removed and TPCK was added to the cells to activate newly synthesized viral particles. Cells were then incubated with media until harvesting at 2, 6, 24, 30, 36 and 48 hpi. For harvesting, the media was first transferred to falcon tubes then we collected cells by the trypsinization followed by centrifugation at 1,500 RPM for 5 minutes at 4ºC. Each pellet was washed with PBS, centrifuged again and stored at -80 ºC. For each infected pellet a non-infected time match control was performed.

D. Reagents and antibodies

The reagents and antibodies that were used in these experiments included reagent A, S and B (Bio-Rad), penicillin 100 units/ml (Gibco), streptomycin 100units/ml (Gibco), isotope-labeled internal standards (Avanti).

E. Lipid extraction

To perform a lipid extraction under a safe neutral condition that avoid destruction of the parent SPLs containing O-acyl groups, the single-phase extraction method was adopted according to Bielawski et al. (2009). This method used ethyl acetate:iso-propanol:water system at 60:30:10; (by volume) for tissue and cell pellets. Briefly, the cell pellets were fortified with 50 ml of appropriate internal standard solutions. The sample were then extracted with 2.0 ml of i–PrOH–Water–EtOAc and centrifuged. Organic upper phase were transferred to a new vial and the samples were re-extracted with an additional 2.0 ml of i–PrOH–Water–EtOAc. After centrifuging, the supernatants were combined and the extracts were dried under nitrogen. The dried residue was re-suspended in a mobile phase and 10µl of the supernatant were injected into a high performance liquid chromatography (HPLC) system.

F. Mass spectrometry LC/MS MS

Sphingolipids quantification is performed using Liquid chromatography/tandem mass spectrometry (LC/MS MS). Mass spectrometry is a detection technique that enables separation and characterization of compounds according to their mass-to-charge ratio (m/z).

Its essential components include a sample inlet, ion source, mass analyzer, detector, and data handling system. Based on the isotope-labeled internal standards used, LC/MS MS was used in order to detect sphingosine, ceramides, sphingomyelins, glucosylceramides, lactosylceramides, and the dihydro-counterparts of each of these classes. Briefly, the samples were pumped through a stationary phase (LC column) by a mobile phase flowing through at high pressure. Chemical interaction between the components of the sample, the stationary phase and the mobile phase affected different migration rates through the LC column and caused a separation. After elution from the LC column, the effluent was directed to the mass spectrometer where it was ionized into charged particles. These charged particles then migrated under high vacuum through a series of mass analyzers known as quadrupole by applying electromagnetic fields. A specific mass/charge precursor ion is targeted to pass through the first quadrupole, excluding all other mass/charge ratio particles. In the second quadrupole also known as the collision cell, the selected mass/charge ions are then fragmented into product ions by collision with an inert gas. The third quadrupole is used to target specific product ion fragments. In the final step, the resulting isolated product ions are quantified with an electron multiplier.

G. Protein extraction and quantification

Cell pellets were resuspended in lysis buffer (0.25 M Tris-HCL, 4% SDS, 20% Glycerol, and 2mg bromophenol blue) supplemented with protease inhibitors (Sigma). The samples were kept 20 minutes on ice, boiled for 5 minutes at 95ºC and centrifuged for 20 minutes at 4ºC. The supernatants were then collected.

The extracted proteins were quantified using Detergent Compatible Bio-Rad Protein Assay (Bio-Rad). Briefly, proteins were mixed with reagent A (alkaline copper tartrate solution) and reagent S followed by reagent B (Folin's reagent) leading to a blue color shade. Using Lowry method, the concentrations of the proteins was determined with respect to a known protein standard concentration of BSA (Amresco).

H. RNA extraction and RT- PCR

Total RNA was extracted using the GenElute Mammalian Total RNA Miniprep Kit (Sigma Aldrich, USA) according to the manufacturer's instructions. Briefly, the samples were lysed using β-mercaptoethanol mixed with lysis solution at a ratio of 1:100. The extracts were passed through a filter via centrifugation, and then equal volumes of 70% ethanol were added to the filtrate. After centrifugation, a series of washing steps were performed, followed by the RNA elution.

Eluted RNA (1µg) was reverse transcribed using the Quantitect Reverse Transcription Kit (QIAGEN, Germany) according to the manufacturer's instructions. Briefly, a mixture of RNA, nuclease-free water, and gDNA wipeout buffer was incubated in a thermal cycler at 42ºC for 2 minutes. The master mix (reverse transcriptase, primer mix, and buffer) was then added to the mixture and the samples were incubated for 30 minutes at 42ºC followed by 3 minutes at 95ºC. Afterwards, the cDNA was diluted to a final concentration of 10ng/µL for real-time PCR experiments.

RT-PCR was performed using Taqman probes and forward/ reverse primers for specific for the genes encoding the ceramide synthase and serine palmitoyl transferase.

I. Statistical analysis

Statistical analysis was done using the GraphPad Prism version 8 software. All data shown are averages of three independent experiments. Quantitative data are expressed as mean ± S.D. Student's t-test (two-tailed) was used for analysis of significance. $P<0.05$ was considered significant.

CHAPTER IV

RESULTS

A. Sphingolipid profile of A549 cells

The first step was to investigate the sphingolipidomic profile of A549 cells in order to identify any differential sphingolipid regulation between the non-infected cells (controls) and the infected ones. Using LC/MS, 71 sphingolipid species were quantified at various time-points (5, 15, 30 minutes and 6, 24, 30, 36, and 48 hpi) in both IAV infected A549 cells and their time-matched controls. The sphingolipid species included sphingosine, sphinganine, ceramides, dihydroceramides, sphingomyelins, dihydrosphingomyelins, gucosylceramides, dihydroglucosylceramides, lactosylceramides, and dihydrolactosylceramides. All measured species had a C18 sphingoid base and their N-acyl chains ranged between C14 and C26 (saturated and unsaturated).

Time matched controls showed that SM and dihydrosphingomyelins are the most abundant species in A549 cells ranging between 92% and 96% with an almost equal ratio of sphingomyelins to dihydrosphingomyelins. Ceramides and glucosylceramides constituted 3% and 1% of the extracted cellular sphingolipids, respectively. Other sphingolipids species including lactosylceramide, sphingosine, sphinganine and dihydroceramide represented less than 1% with the sphingosine marking the highest abundancy (Figure 9, A; B).

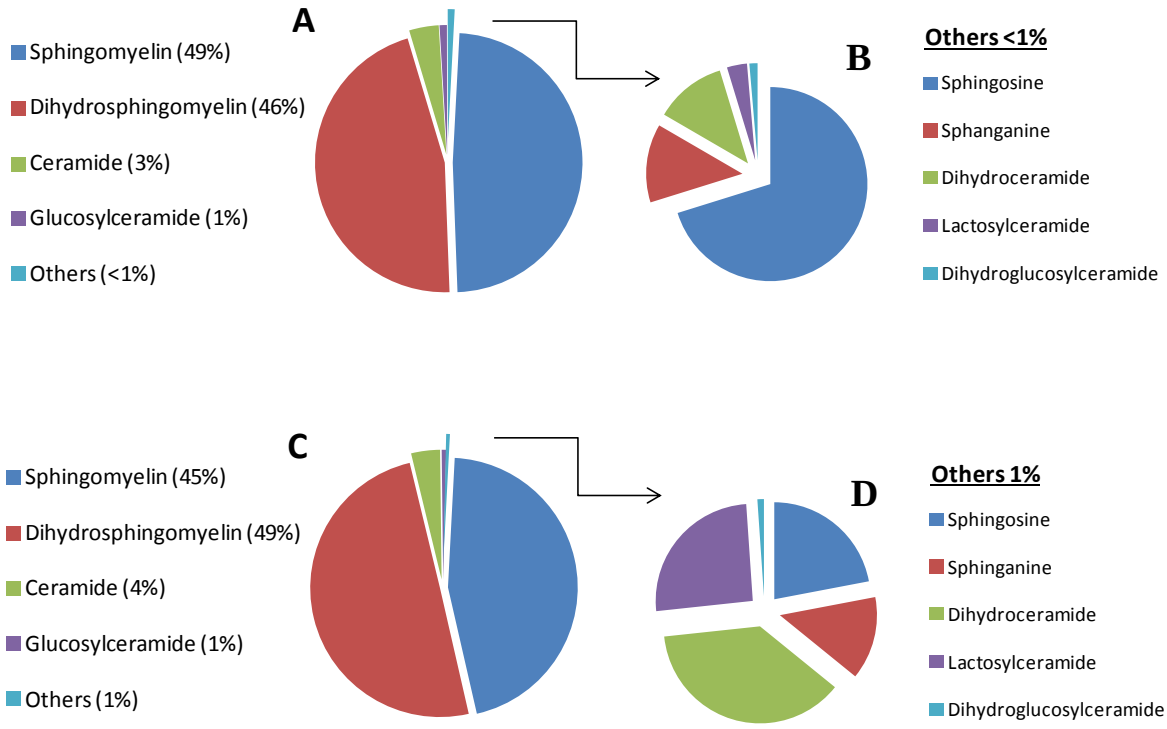

Figure 9. Sphingolipid profiling of non-infected versus IAV-infected A549 cells
(A) SM and dihydrosphingomyelin represent 95% of A549 cellular sphingolipids while ceramide and glucosylceramide represent 3% and 1%, respectively. (B) Other sphingolipids represent less than 1%. (C) SM and dihydrosphingomyelin represent 94% of A549 cellular sphingolipids in infected cells while ceramide and glucosylceramide represent 4% and 1%, respectively. (D) Other sphingolipids represent 1%.

B. IAV alters the ceramide metabolism

An assessment of ceramide levels was performed. Results indicated that pooled ceramide levels increased starting 30 hpi and continued to rise at 48 hpi, however, not significantly (data not shown). Among the ceramide species, d18:1/d16:0, d18:1/d20:1 and d18:1/d22:1 were the major species that increased significantly at 36 hpi in IAV infected

cells compared to time matched controls (Mock) (Figure 10: A; B; C). d18:1/ d16:0 continued to increase at 48 hpi in infected cells (Figure 10: A).

Next, dihydroceramides generated from sphinganine in the *de novo* pathway by ceramide synthases were assessed. Results indicate that total dihydroceramides increased starting at 24 hpi in IAV infected cells and continued to rise until 48 hpi (data not shown).

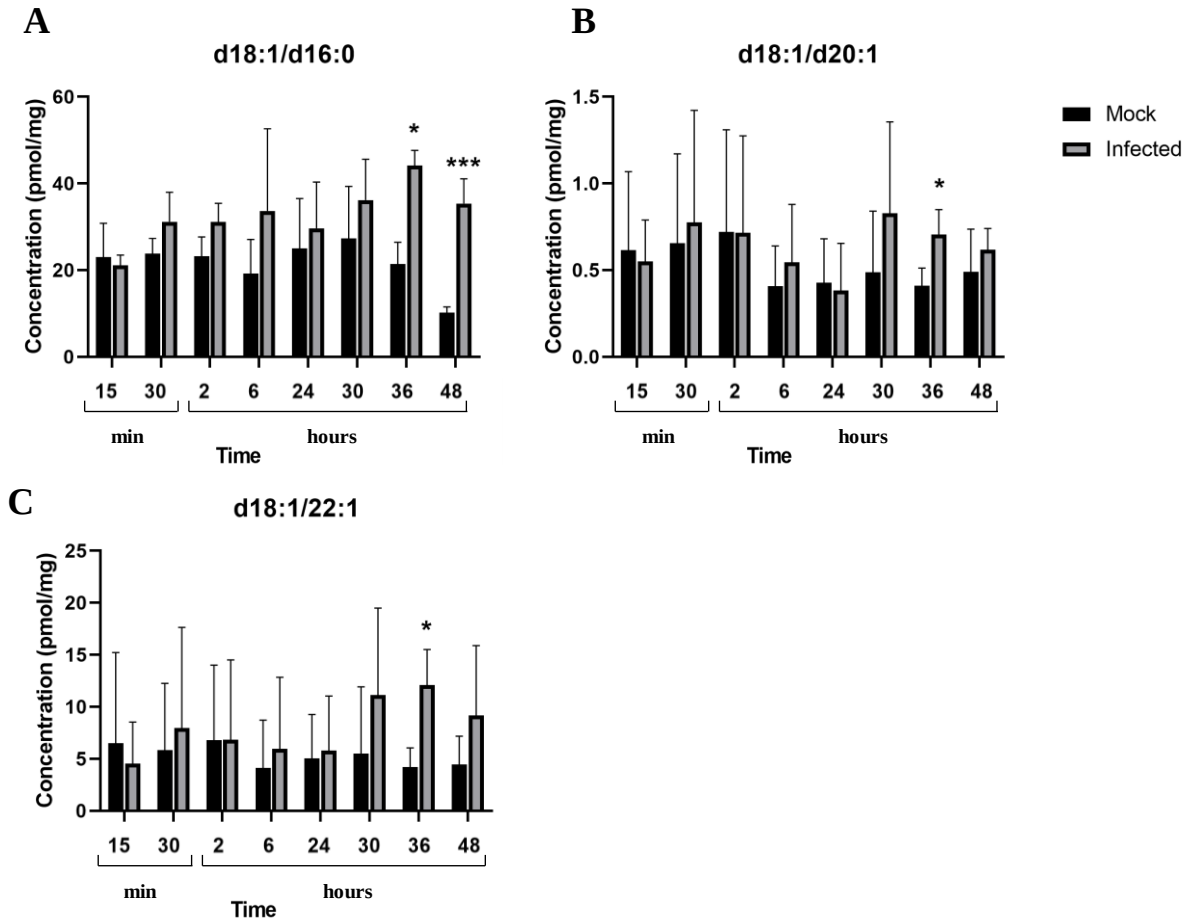

Figure 10. Regulation of ceramide species upon IAV infection.
Data are presented as mean ± S.D of infected and non-infected controls. *P<0.05. ***P<0.001
(A) d18:1/d16:0 levels. (B) d18:1/d18:1 levels. (C) d18:1/d22:1 levels.

C. IAV downregulated SM species

The whole profile of the SM and dihydrosphingomyelin were not changed upon IAV infection, yet some individual SM species were significantly downregulated at later time points in IAV infected cells. C18:1-SM species were significantly decreased at 48 hpi (Figure 11: A) while C24-SM and C26-SM were significantly downregulated at 36 hpi (Figure 11: B; C).

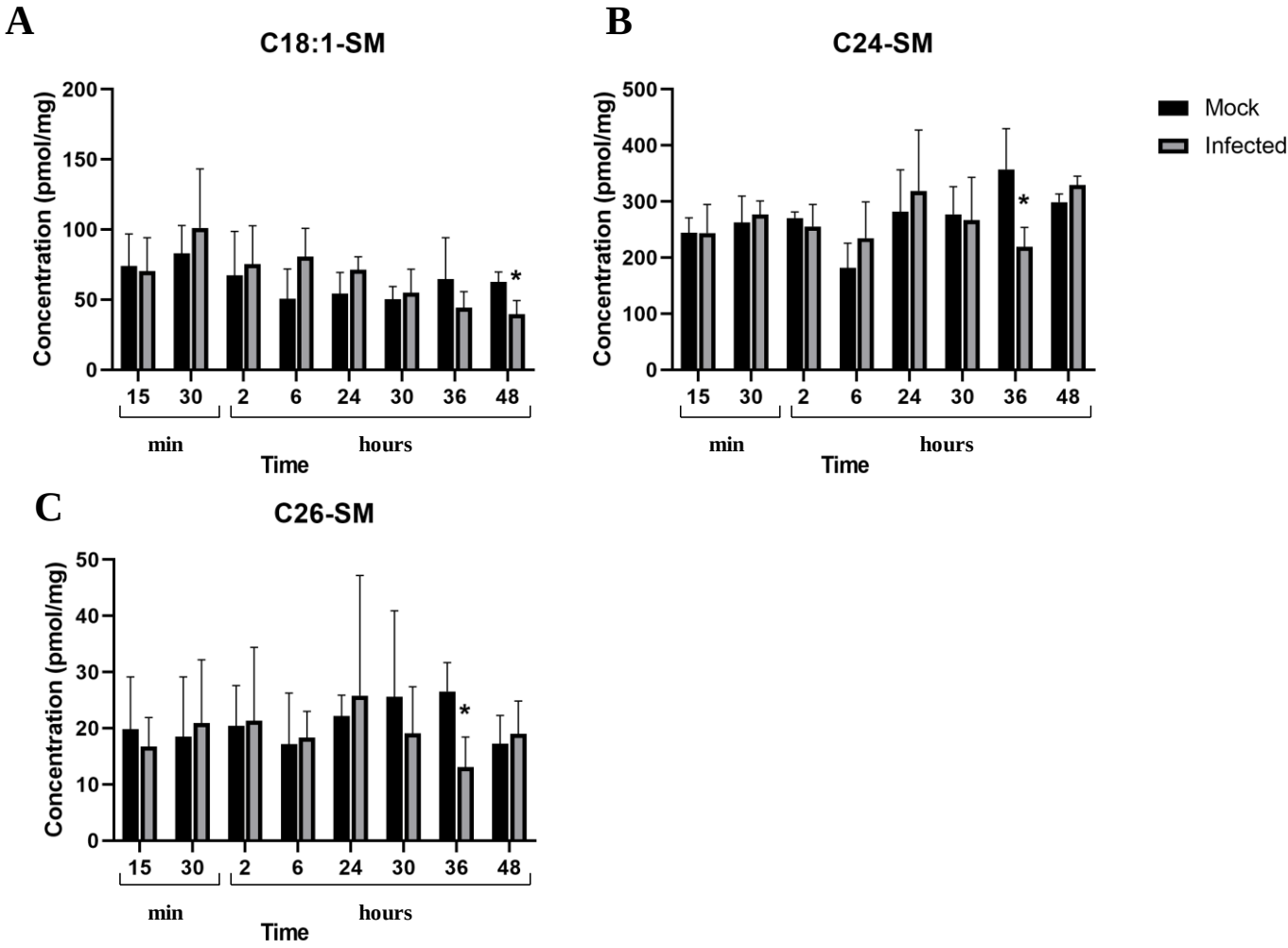

Figure 11. Regulation of SM species upon influenza A virus infection.

LC/MS was used to quantify SM species in infected and non-infected A549 cells. Data are presented as mean ± S.D. *$P<0.05$.

D. IAV significantly increases lactosylceramide in infected A549 cells

While total glucosylceramide and dihydroglucosylceramide in infected versus non-infected A549 cells were not altered upon IAV infection (data not shown), lactosylceramide, which is the catabolic product of glucosylceramide, was elevated starting at 24 hpi. The significant increase was detected at 36 and 48 hpi (Figure 12: A).

The C16-Lact-Cer was the only lactosylceramide species that started to increase at 24 hpi and showed a significant rise at both 36 hpi and 48 hpi (Figure 12: B). The remaining lactosylceramide species were unaltered (data not shown).

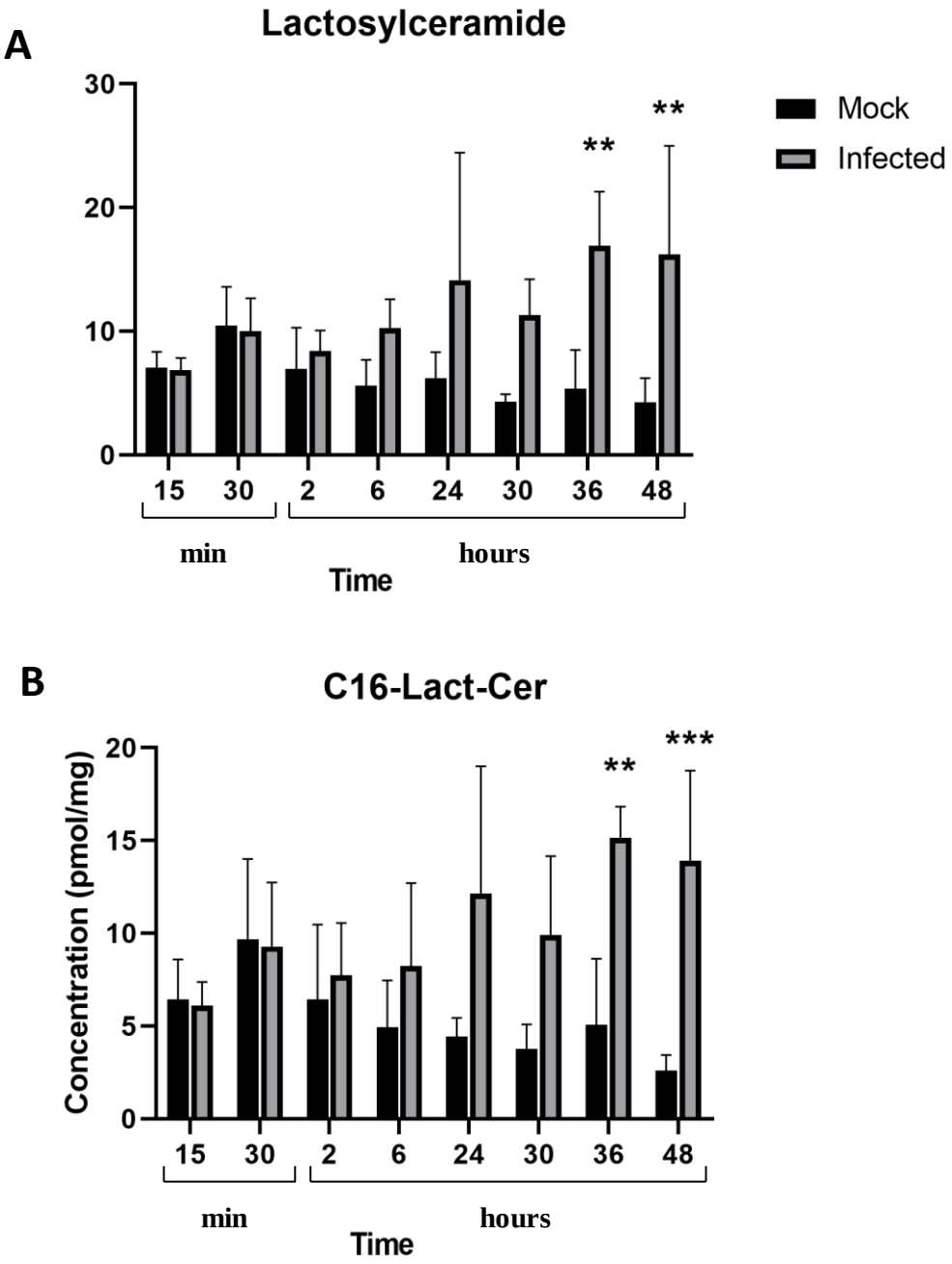

Figure 12. Regulation of total lactosylceramide and C16-Lactosylceramide levels upon IAV infection.
(A) LC/MS was used to quantify total lactosylceramide in both infected and non-infected A549 cells. (B) C16-Lactosylceramide levels. Data are presented as mean ± S.D. **P<0.01;***P<0.001.

E. IAV regulates the gene expression of key enzymes involved in *de novo* ceramide synthesis

Different enzymes involved in the *de novo* pathway of ceramide synthesis were quantified using RT-PCR. These data were previously generated by Dr Nadia Soudani in Zaraket laboratory. The results showed an overexpression in *CerS1*, *CerS2*, *CerS4* and *CerS6* starting 36 hpi (Figure 13). Interestingly, CerS1 and CerS4 were shown mainly to be responsible for generating C18 and C20 ceramide while CerS6 for generating C16 [132, 133], the same species that were upregulated in our IAV-infected cells. Due to several limitations, we were unable to continue the study of other enzymes expression levels involved in other ceramide biosynthetic pathways.

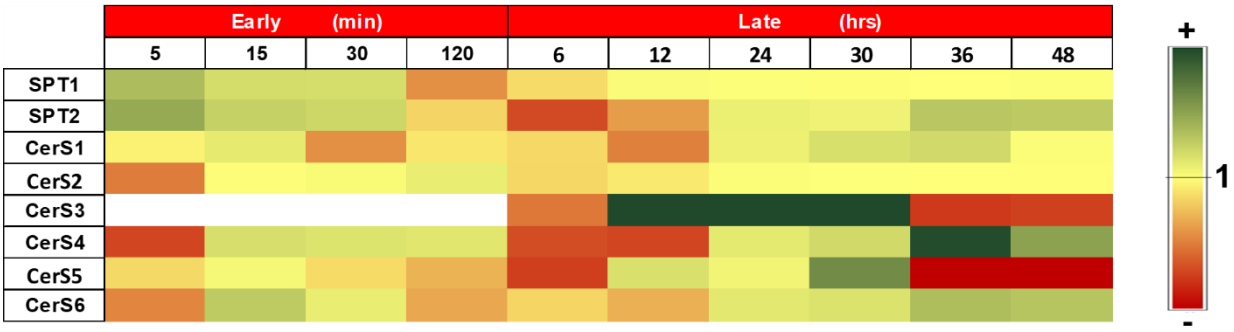

Figure 13. Regulation of gene expression of key enzymes involved in *de novo* ceramide synthesis in response to IAV infection

CHAPTER V

DISCUSSION

In this study, an LC/MS based sphingolipidomics approach was utilized in order to establish a detailed lipid profile of infected human lung epithelial cell line A549 with IAV and determine the impact of IAV infection on cellular sphingolipid metabolism. IAV is an enveloped virus that infects epithelial cells. As it hijacks the host cellular machinery and impacts host cell metabolism to tailor cellular pathways and resources to their needs for efficient replication, assembly and budding, newly synthesized viral particles tend to build its envelope from the host membrane, where sphingolipids are key components [134, 135]. Sphingolipids are a complex group of lipids that regulate apoptosis, cell-cycle arrest, differentiation, migration, proliferation, and senescence [136]. Ceramide is the central metabolite in the sphingolipid network and it serves as a metabolic and structural precursor for complex sphingolipids. It can be generated either via the *de novo* pathway, sphingomyelin hydrolysis, or alternatively via the salvage pathway [137].

Previous studies showed that IAV have the capacity to actively remodel the lipid host landscape by tuning cellular sphingolipids and regulating different ceramide species [54]. Our results showed that IAV infection triggered the increase of several ceramide species despite that the total ceramide levels were slightly altered. In a previous study, ceramide levels increased in response to IAV infection in a dose- and time-dependent manner mainly mediated through the *de novo* biosynthesis pathway [10]. Ceramide levels were previously assessed by DGK assay in which both ceramide and dihydroceramide are

phosphorylated by diacyglycerol kinase in the presence of radioactive labeled ATP. The DGK assay suffers from its inability to distinguish between ceramides and dihydroceramides. In the current work, the total ceramide and dihydroceramide levels were calculated as the sum of all detected species and were shown to be slightly altered upon infection. Individual species were increasing significantly such as d18:1/d16:0, d18:1/d20:1 and d18:1/d22:1. Noting that significant cell death was observed in IAV infected cells 48 hours post-infection (unpublished data), C16-ceramide was significantly increased 36 and 48 hours post IAV infection and potentially drove pro-apoptotic response to IAV infection [138]. Moreover, C18- and C20-ceramides were also elevated and were shown to have antiviral roles against several viruses like measles viruses and human immunodeficiency virus (HIV) [139].

Influenza virus requires a functional SM synthesis pathway for the generation of infectious particles [130]. In addition to influenza virus, SM and ASmase were shown to influence cell entry of a number of viruses. Ebola virus requires the host cell plasma membrane SM and ASmase activity for successful infection [140]. Moreover, West Nile virus infection is enhanced by SM accumulation and is decreased by depletion of SM. Hepatitis C virus requires viral envelope SM and cholesterol for successful infection [141]. Alphaherpesviruses were shown to exhibit a variable requirement for SM and ASMase during entry into host cells [142] . In our model, SM and dihydrosphingomyelin constitute approximately 94% of the A549 cellular sphingolipids. According to Audi et al. [131], SM was required in both cell membrane and viral envelope for an efficient virus entry as well as host cell's SM was seen to promote IAV replication. Furthermore, IAV infection was

associated with a significant decrease in ASMase activity 24 and 48 hpi [131]. This study suggests that IAV inhibited ASMase activity at later stages of infection to preserve SM for subsequent infection cycles. In our study, SM levels were not affected after IAV infection although some SM species such as C18:1-SM, C24-SM and C26-SM were significantly downregulated at late time points (36 and 48 hpi). This might be explained by the fact that SM could be altered after several replication IAV cycles. A potential role for N-Smase is being currently investigated in our laboratory.

Glucosylceramide synthase, which synthesizes glucosylceramide from ceramide, was shown to be necessary for proper virus entry. In fact, knocking out glucosylceramide synthase decreased GlcCer levels (in both HEK 293 and A549 cells), thereby impairing the entry of endosome-entering viruses [122], yet our results did not show any alteration of glucosylceramide in IAV-infected cells versus controls. In fact, cells might be trying to maintain a state of glucosylceramide homeostasis upon infection to promote virus entry. Interestingly, lactosylceramide was significantly overexpressed at late time points and specifically the C16-lactosylceramide. This still needs further investigations as the lactosylceramide is a minor species in which minimal perturbations in its levels could have significant biological outcomes. [143]. IAV was shown to induce apoptosis [144] and this might be through lactosylceramide since lactosylceramide was shown to play a critical role in inducing apoptosis mainly through N-SMase [145].

The intact levels of sphingosine observed during IAV infected cells may be explained by the conversion of sphingosine into S1P via the action of sphingosine kinase. A recent study suggested that S1P might be increasing in favor of the virus replication post-

infection [1]. Unfortunately, LC/MS was unable to detect S1P in our model, despite the favorable method of lipid extraction used. This is likely due to the sub-picomole expression levels of S1P, and hence an evaded detection. On the other hand, the cell might be shutting the ceramide catabolism pathway to accumulate ceramide since sphingosine degradation into S1P is irreversible [146]. Moreover, ceramide synthases, which are present in the ER, are able to generate ceramides directly from sphingosine [147]. Unpublished data from our laboratory showed an overexpression in *CerS1, CerS2, CerS4* and *CerS6* starting 36 hpi. Interestingly, CerS1 and CerS4 were shown mainly to be responsible for generating C18 and C20 ceramide while CerS6 for generating C16 [132, 133], the same species that were upregulated in our IAV infected cells.

The major sphingolipid pathways that regulate ceramide synthesis during IAV needs further investigations. In fact, it is hypothesized the *de novo* pathway could be a major driver of the observed perturbation in sphingolipid levels since it modulates the infectivity and the replication of different viruses. similarly to previous data from our laboratory [10], the ceramide production via the *de novo* pathway is a requirement for West Nile virus, HCV and HIV virus replication [148, 149].

CHAPTER VI

CONCLUSION

In this study, we have shown that the IAV induces sphingolipid alterations in lung epithelial cells, especially in ceramide, sphingomyelin and lactosylceramide species. IAV did not alter all sphingolipids metabolic products and this could be due to cell host response to counteract the IAV infection. Whether the ceramide accumulation is exclusively driven by the *de* novo pathway or could be accompanied by other ceramide biosynthetic pathway such as the salvage pathway is still unclear at this point. Further investigations will be conducted.

CHAPTER VII

FUTURE PERSPECTIVES

Several experiments will be performed in order to investigate how the ceramide is involved in the host defense mechanism against IAV and how it counters to survive. On the other hand, we will study how the virus could modulate the host response on its favor to complete proper life cycle using different sphingolipids.

LC/MS will be applied also on IAV infected cells upon inhibition with different enzyme inhibitors to decipher which biosynthetic pathway is involved post IAV infection.

REFERENCES

1. Seo, Y.J., et al., *Sphingosine 1-phosphate-metabolizing enzymes control influenza virus propagation and viral cytopathogenicity.* J Virol, 2010. **84**(16): p. 8124-31.
2. Rash, A., et al., *An efficient genome sequencing method for equine influenza [H3N8] virus reveals a new polymorphism in the PA-X protein.* Virology Journal, 2014. **11**(1): p. 159.
3. Seo, Y.-J., et al., *Sphingosine Kinase 1 Serves as a Pro-Viral Factor by Regulating Viral RNA Synthesis and Nuclear Export of Viral Ribonucleoprotein Complex upon Influenza Virus Infection.* PLOS ONE, 2013. **8**(8): p. e75005.
4. Hause, B.M., et al., *Characterization of a novel influenza virus in cattle and Swine: proposal for a new genus in the Orthomyxoviridae family.* mBio, 2014. **5**(2): p. e00031-14.
5. Hurt, A.C., et al., *Evidence for the Introduction, Reassortment, and Persistence of Diverse Influenza A Viruses in Antarctica.* J Virol, 2016. **90**(21): p. 9674-9682.
6. Tsai, C.P. and H.J. Tsai, *Influenza B viruses in pigs, Taiwan.* Influenza Other Respir Viruses, 2019. **13**(1): p. 91-105.
7. Richard, M., et al., *Influenza A viruses are transmitted via the air from the nasal respiratory epithelium of ferrets.* Nat Commun, 2020. **11**(1): p. 766.
8. Chughtai, A.A., et al., *The presence of fever in adults with influenza and other viral respiratory infections.* Epidemiol Infect, 2017. **145**(1): p. 148-155.
9. Wang, W., et al., *Human antibody 3E1 targets the HA stem region of H1N1 and H5N6 influenza A viruses.* Nat Commun, 2016. **7**: p. 13577.
10. Soudani, N., et al., *Ceramide Suppresses Influenza A Virus Replication In Vitro.* Journal of Virology, 2019. **93**(7): p. 01.
11. Yang, H., et al., *Structure and receptor binding preferences of recombinant human A(H3N2) virus hemagglutinins.* Virology, 2015. **477**: p. 18-31.
12. Zhong, J., et al., *Genetic mutations in influenza H3N2 viruses from a 2012 epidemic in Southern China.* Virology Journal, 2013. **10**(1): p. 345.
13. Dam, S., et al., *The Influenza A Virus Genotype Determines the Antiviral Function of NF-kappaB.* J Virol, 2016. **90**(17): p. 7980-90.
14. Lin, R.W., et al., *Naturally occurring mutations in PB1 affect influenza A virus replication fidelity, virulence, and adaptability.* J Biomed Sci, 2019. **26**(1): p. 55.
15. Germeraad, E., et al., *The development of a multiplex serological assay for avian influenza based on Luminex technology.* Methods, 2019. **158**: p. 54-60.
16. Wei, F., et al., *Induction of PGRN by influenza virus inhibits the antiviral immune responses through downregulation of type I interferons signaling.* PLoS Pathog, 2019. **15**(10): p. e1008062.
17. Krammer, F., et al., *Influenza.* Nature Reviews Disease Primers, 2018. **4**(1): p. 3.
18. Li, W., et al., *Interactions between the influenza A virus RNA polymerase components and retinoic acid-inducible gene I.* J Virol, 2014. **88**(18): p. 10432-47.
19. Chou, Y.Y., et al., *One influenza virus particle packages eight unique viral RNAs as shown by FISH analysis.* Proc Natl Acad Sci U S A, 2012. **109**(23): p. 9101-6.

20. Ma, J., et al., *Effects of the PA-X and PB1-F2 Proteins on the Virulence of the 2009 Pandemic H1N1 Influenza A Virus in Mice.* Front Cell Infect Microbiol, 2019. **9**: p. 315.
21. Yamayoshi, S., et al., *Identification of a Novel Viral Protein Expressed from the PB2 Segment of Influenza A Virus.* J Virol, 2016. **90**(1): p. 444-56.
22. Rossman, J.S., G.P. Leser, and R.A. Lamb, *Filamentous influenza virus enters cells via macropinocytosis.* J Virol, 2012. **86**(20): p. 10950-60.
23. Elton, D., et al., *The genetics of virus particle shape in equine influenza A virus.* Influenza Other Respir Viruses, 2013. **7 Suppl 4**: p. 81-9.
24. Tanner, L.B., et al., *Lipidomics identifies a requirement for peroxisomal function during influenza virus replication.* J Lipid Res, 2014. **55**(7): p. 1357-65.
25. Gerl, M.J., et al., *Quantitative analysis of the lipidomes of the influenza virus envelope and MDCK cell apical membrane.* J Cell Biol, 2012. **196**(2): p. 213-21.
26. Lopez-Martinez, R., et al., *Inhibition of influenza A virus infection in vitro by peptides designed in silico.* PLoS One, 2013. **8**(10): p. e76876.
27. Chen, F., et al., *Key amino acid residues of neuraminidase involved in influenza A virus entry.* Pathog Dis, 2019. **77**(6).
28. Liu, H., M.L. Grantham, and A. Pekosz, *Mutations in the Influenza A Virus M1 Protein Enhance Virus Budding To Complement Lethal Mutations in the M2 Cytoplasmic Tail.* Journal of virology, 2017. **92**(1): p. e00858-17.
29. Calder, L.J., et al., *Structural organization of a filamentous influenza A virus.* Proc Natl Acad Sci U S A, 2010. **107**(23): p. 10685-90.
30. Su, W.C., et al., *Ubiquitination of the Cytoplasmic Domain of Influenza A Virus M2 Protein Is Crucial for Production of Infectious Virus Particles.* J Virol, 2018. **92**(4).
31. Wang, S., et al., *Identification of two residues within the NS1 of H7N9 influenza A virus that critically affect the protein stability and function.* Vet Res, 2018. **49**(1): p. 98.
32. Hu, Y., et al., *CHD3 facilitates vRNP nuclear export by interacting with NES1 of influenza A virus NS2.* Cell Mol Life Sci, 2015. **72**(5): p. 971-82.
33. Nelson, M.I. and E.C. Holmes, *The evolution of epidemic influenza.* Nat Rev Genet, 2007. **8**(3): p. 196-205.
34. Watanabe, K., et al., *Nuclear export of the influenza virus ribonucleoprotein complex: Interaction of Hsc70 with viral proteins M1 and NS2.* FEBS Open Bio, 2014. **4**: p. 683-8.
35. Das, D.K., et al., *Direct Visualization of the Conformational Dynamics of Single Influenza Hemagglutinin Trimers.* Cell, 2018. **174**(4): p. 926-937 e12.
36. Anderson, C.S., et al., *Natural and directed antigenic drift of the H1 influenza virus hemagglutinin stalk domain.* Sci Rep, 2017. **7**(1): p. 14614.
37. Leung, H.S., et al., *Entry of influenza A Virus with a alpha2,6-linked sialic acid binding preference requires host fibronectin.* J Virol, 2012. **86**(19): p. 10704-13.
38. Drews, K., et al., *Glucosylceramidase Maintains Influenza Virus Infection by Regulating Endocytosis.* Journal of Virology, 2019. **93**(12): p. e00017-19.
39. Sakai, T., et al., *Influenza A virus hemagglutinin and neuraminidase act as novel motile machinery.* Sci Rep, 2017. **7**: p. 45043.

40. Akole, A. and J.M. Warner, *Model of influenza virus acidification.* PLoS One, 2019. **14**(4): p. e0214448.
41. Heldt, F.S., T. Frensing, and U. Reichl, *Modeling the intracellular dynamics of influenza virus replication to understand the control of viral RNA synthesis.* J Virol, 2012. **86**(15): p. 7806-17.
42. Wu, W., et al., *Synergy of two low-affinity NLSs determines the high avidity of influenza A virus nucleoprotein NP for human importin alpha isoforms.* Sci Rep, 2017. **7**(1): p. 11381.
43. Perez, D.R., et al., *Phospholipid scramblase 1 interacts with influenza A virus NP, impairing its nuclear import and thereby suppressing virus replication.* PLOS Pathogens, 2018. **14**(1).
44. Chen, K.Y., et al., *Influenza virus polymerase subunits co-evolve to ensure proper levels of dimerization of the heterotrimer.* PLoS Pathog, 2019. **15**(10): p. e1008034.
45. Nilsson, B.E., A.J.W. Te Velthuis, and E. Fodor, *Role of the PB2 627 Domain in Influenza A Virus Polymerase Function.* J Virol, 2017. **91**(7).
46. Robb, N.C., et al., *Single-molecule FRET reveals the pre-initiation and initiation conformations of influenza virus promoter RNA.* Nucleic Acids Res, 2016. **44**(21): p. 10304-10315.
47. York, A., et al., *Isolation and characterization of the positive-sense replicative intermediate of a negative-strand RNA virus.* Proc Natl Acad Sci U S A, 2013. **110**(45): p. E4238-45.
48. Rialdi, A., et al., *The RNA Exosome Syncs IAV-RNAPII Transcription to Promote Viral Ribogenesis and Infectivity.* Cell, 2017. **169**(4): p. 679-692 e14.
49. Reich, S., et al., *Structural insight into cap-snatching and RNA synthesis by influenza polymerase.* Nature, 2014. **516**(7531): p. 361-6.
50. Sasaki, K., et al., *Characterization of a novel mutation in NS1 protein of influenza A virus induced by a chemical substance for the attenuation of pathogenicity.* PLoS One, 2015. **10**(3): p. e0121205.
51. Cheng, J., et al., *Effects of the S42 residue of the H1N1 swine influenza virus NS1 protein on interferon responses and virus replication.* Virol J, 2018. **15**(1): p. 57.
52. Tynell, J., K. Melén, and I. Julkunen, *Mutations within the conserved NS1 nuclear export signal lead to inhibition of influenza A virus replication.* Virology Journal, 2014. **11**(1): p. 128.
53. Trigueiro-Louro, J.M., et al., *To hit or not to hit: Large-scale sequence analysis and structure characterization of influenza A NS1 unlocks new antiviral target potential.* Virology, 2019. **535**: p. 297-307.
54. Vale-Costa, S., et al., *Influenza A virus ribonucleoproteins modulate host recycling by competing with Rab11 effectors.* J Cell Sci, 2016. **129**(8): p. 1697-710.
55. de Castro Martin, I.F., et al., *Influenza virus genome reaches the plasma membrane via a modified endoplasmic reticulum and Rab11-dependent vesicles.* Nat Commun, 2017. **8**(1): p. 1396.
56. Kawaguchi, A., et al., *Influenza Virus Induces Cholesterol-Enriched Endocytic Recycling Compartments for Budozone Formation via Cell Cycle-Independent Centrosome Maturation.* PLoS Pathog, 2015. **11**(11): p. e1005284.

57. Sato, R., et al., *Apical Trafficking Pathways of Influenza A Virus HA and NA via Rab17- and Rab23-Positive Compartments.* Front Microbiol, 2019. **10**: p. 1857.
58. Vahey, M.D. and D.A. Fletcher, *Influenza A virus surface proteins are organized to help penetrate host mucus.* Elife, 2019. **8**.
59. Eisfeld, A.J., G. Neumann, and Y. Kawaoka, *At the centre: influenza A virus ribonucleoproteins.* Nat Rev Microbiol, 2015. **13**(1): p. 28-41.
60. Saito, R., et al., *High prevalence of amantadine-resistance influenza a (H3N2) in six prefectures, Japan, in the 2005-2006 season.* J Med Virol, 2007. **79**(10): p. 1569-76.
61. Hussein, A.F.A., et al., *Identification of entry inhibitors with 4-aminopiperidine scaffold targeting group 1 influenza A virus.* Antiviral Res, 2020. **177**: p. 104782.
62. O'Hanlon, R. and M.L. Shaw, *Baloxavir marboxil: the new influenza drug on the market.* Curr Opin Virol, 2019. **35**: p. 14-18.
63. Ilyushina, N.A., et al., *Combination chemotherapy, a potential strategy for reducing the emergence of drug-resistant influenza A variants.* Antiviral Res, 2006. **70**(3): p. 121-31.
64. Basu, A., et al., *New small molecule entry inhibitors targeting hemagglutinin-mediated influenza a virus fusion.* J Virol, 2014. **88**(3): p. 1447-60.
65. *<A-Bielawski2009_Protocol_ComprehensiveQuantita.pdf>*.
66. Kanyiri, C.W., K. Mark, and L. Luboobi, *Mathematical Analysis of Influenza A Dynamics in the Emergence of Drug Resistance.* Comput Math Methods Med, 2018. **2018**: p. 2434560.
67. Ma, C., et al., *Discovery of cyclosporine A and its analogs as broad-spectrum anti-influenza drugs with a high in vitro genetic barrier of drug resistance.* Antiviral Res, 2016. **133**: p. 62-72.
68. Rogers, M.B., et al., *Intrahost dynamics of antiviral resistance in influenza A virus reflect complex patterns of segment linkage, reassortment, and natural selection.* mBio, 2015. **6**(2).
69. Hauge, S.H., et al., *Oseltamivir-resistant influenza viruses A (H1N1), Norway, 2007-08.* Emerg Infect Dis, 2009. **15**(2): p. 155-62.
70. Wu, Y., et al., *Resistance to Mutant Group 2 Influenza Virus Neuraminidases of an Oseltamivir-Zanamivir Hybrid Inhibitor.* J Virol, 2016. **90**(23): p. 10693-10700.
71. Kurebayashi, Y., et al., *High-Efficiency Capture of Drug Resistant-Influenza Virus by Live Imaging of Sialidase Activity.* PLoS One, 2016. **11**(5): p. e0156400.
72. Moasser, E., A. Moasser, and H. Zaraket, *Incidence of antiviral drug resistance markers among human influenza A viruses in the Eastern Mediterranean Region, 2005-2016.* Infect Genet Evol, 2019. **67**: p. 60-66.
73. An, D., et al., *Membrane sphingolipids as essential molecular signals for Bacteroides survival in the intestine.* Proc Natl Acad Sci U S A, 2011. **108 Suppl 1**: p. 4666-71.
74. Li, G., et al., *Efficient replacement of plasma membrane outer leaflet phospholipids and sphingolipids in cells with exogenous lipids.* Proc Natl Acad Sci U S A, 2016. **113**(49): p. 14025-14030.
75. Snider, J.M., et al., *Probing de novo sphingolipid metabolism in mammalian cells utilizing mass spectrometry.* J Lipid Res, 2018. **59**(6): p. 1046-1057.

76. Melland-Smith, M., et al., *Disruption of sphingolipid metabolism augments ceramide-induced autophagy in preeclampsia.* Autophagy, 2015. **11**(4): p. 653-69.
77. Sakamoto, W., et al., *Probing compartment-specific sphingolipids with targeted bacterial sphingomyelinases and ceramidases.* Journal of lipid research, 2019. **60**(11): p. 1841-1850.
78. SG, B.G., K. Ikeda, and M. Arita, *Facile determination of sphingolipids under alkali condition using metal-free column by LC-MS/MS.* Anal Bioanal Chem, 2018. **410**(20): p. 4793-4803.
79. Parra-Lobato, M.C., et al., *Localization of Sphingolipid Enriched Plasma Membrane Regions and Long-Chain Base Composition during Mature-Fruit Abscission in Olive.* Front Plant Sci, 2017. **8**: p. 1138.
80. Blackburn, N.B., et al., *Rare DEGS1 variant significantly alters de novo ceramide synthesis pathway.* Journal of lipid research, 2019. **60**(9): p. 1630-1639.
81. Maceyka, M. and S. Spiegel, *Sphingolipid metabolites in inflammatory disease.* Nature, 2014. **510**(7503): p. 58-67.
82. Wronowska, W., et al., *Computational modeling of sphingolipid metabolism.* BMC Syst Biol, 2015. **9**: p. 47.
83. Husari, A.W., et al., *Apoptosis and the activity of ceramide, Bax and Bcl-2 in the lungs of neonatal rats exposed to limited and prolonged hyperoxia.* Respir Res, 2006. **7**: p. 100.
84. Dadsena, S., et al., *Ceramides bind VDAC2 to trigger mitochondrial apoptosis.* Nat Commun, 2019. **10**(1): p. 1832.
85. Panjarian, S., et al., *De novo N-palmitoylsphingosine synthesis is the major biochemical mechanism of ceramide accumulation following p53 up-regulation.* Prostaglandins Other Lipid Mediat, 2008. **86**(1-4): p. 41-8.
86. Pinto, S.N., et al., *Effect of ceramide structure on membrane biophysical properties: the role of acyl chain length and unsaturation.* Biochim Biophys Acta, 2011. **1808**(11): p. 2753-60.
87. Ji, R., et al., *Increased de novo ceramide synthesis and accumulation in failing myocardium.* JCI Insight, 2017. **2**(9).
88. Shamseddine, A.A., et al., *P53-dependent upregulation of neutral sphingomyelinase-2: role in doxorubicin-induced growth arrest.* Cell Death Dis, 2015. **6**: p. e1947.
89. Chavez, J.A., et al., *Ceramides and glucosylceramides are independent antagonists of insulin signaling.* J Biol Chem, 2014. **289**(2): p. 723-34.
90. Zabielski, P., et al., *Effect of plasma free fatty acid supply on the rate of ceramide synthesis in different muscle types in the rat.* PLoS One, 2017. **12**(11): p. e0187136.
91. Tafesse, F.G., et al., *Sphingomyelin synthase-related protein SMSr is a suppressor of ceramide-induced mitochondrial apoptosis.* J Cell Sci, 2014. **127**(Pt 2): p. 445-54.
92. Lin, M.H., et al., *Fatty acid transport protein 4 is required for incorporation of saturated ultralong-chain fatty acids into epidermal ceramides and monoacylglycerols.* Sci Rep, 2019. **9**(1): p. 13254.

93. Maula, T., M.A. Al Sazzad, and J.P. Slotte, *Influence of Hydroxylation, Chain Length, and Chain Unsaturation on Bilayer Properties of Ceramides.* Biophys J, 2015. **109**(8): p. 1639-51.
94. Becam, J., et al., *Antibacterial activity of ceramide and ceramide analogs against pathogenic Neisseria.* Sci Rep, 2017. **7**(1): p. 17627.
95. Fekry, B., et al., *C16-ceramide is a natural regulatory ligand of p53 in cellular stress response.* Nat Commun, 2018. **9**(1): p. 4149.
96. Goldfinger, M., et al., *De novo ceramide synthesis is required for N-linked glycosylation in plasma cells.* J Immunol, 2009. **182**(11): p. 7038-47.
97. Hullin-Matsuda, F., et al., *Limonoid compounds inhibit sphingomyelin biosynthesis by preventing CERT protein-dependent extraction of ceramides from the endoplasmic reticulum.* J Biol Chem, 2012. **287**(29): p. 24397-411.
98. Ren, J., et al., *Quantification of 3-ketodihydrosphingosine using HPLC-ESI-MS/MS to study SPT activity in yeast Saccharomyces cerevisiae.* J Lipid Res, 2018. **59**(1): p. 162-170.
99. Blachnio-Zabielska, A., et al., *Reduction of ceramide de novo synthesis in solid tissues changes sphingolipid levels in rat plasma, erythrocytes and platelets.* Adv Med Sci, 2016. **61**(1): p. 72-7.
100. Wigger, D., et al., *Monitoring the Sphingolipid de novo Synthesis by Stable-Isotope Labeling and Liquid Chromatography-Mass Spectrometry.* Front Cell Dev Biol, 2019. **7**: p. 210.
101. Alsanafi, M., et al., *Native and Polyubiquitinated Forms of Dihydroceramide Desaturase Are Differentially Linked to Human Embryonic Kidney Cell Survival.* Mol Cell Biol, 2018. **38**(23).
102. Reali, F., et al., *Mechanistic interplay between ceramide and insulin resistance.* Sci Rep, 2017. **7**: p. 41231.
103. Turner, N., et al., *A selective inhibitor of ceramide synthase 1 reveals a novel role in fat metabolism.* Nat Commun, 2018. **9**(1): p. 3165.
104. Azzam, R., et al., *Regulation of de novo ceramide synthesis: the role of dihydroceramide desaturase and transcriptional factors NFATC and Hand2 in the hypoxic mouse heart.* DNA Cell Biol, 2013. **32**(6): p. 310-9.
105. Kurek, K., et al., *Inhibition of ceramide de novo synthesis with myriocin affects lipid metabolism in the liver of rats with streptozotocin-induced type 1 diabetes.* Biomed Res Int, 2014. **2014**: p. 980815.
106. Bandet, C.L., et al., *Ceramide Transporter CERT Is Involved in Muscle Insulin Signaling Defects Under Lipotoxic Conditions.* Diabetes, 2018. **67**(7): p. 1258-1271.
107. Liu, L.K., et al., *An inducible ER-Golgi tether facilitates ceramide transport to alleviate lipotoxicity.* J Cell Biol, 2017. **216**(1): p. 131-147.
108. Palau, V.E., et al., *gamma-Tocotrienol induces apoptosis in pancreatic cancer cells by upregulation of ceramide synthesis and modulation of sphingolipid transport.* BMC Cancer, 2018. **18**(1): p. 564.
109. Chen, P.W., et al., *Dynamics of the Heat Stress Response of Ceramides with Different Fatty-Acyl Chain Lengths in Baker's Yeast.* PLoS Comput Biol, 2015. **11**(8): p. e1004373.

110. Halasiddappa, L.M., et al., *Oxidized phospholipids induce ceramide accumulation in RAW 264.7 macrophages: role of ceramide synthases.* PLoS One, 2013. **8**(7): p. e70002.
111. Gustafsson, K., et al., *Potentiation of cannabinoid-induced cytotoxicity in mantle cell lymphoma through modulation of ceramide metabolism.* Mol Cancer Res, 2009. **7**(7): p. 1086-98.
112. Morad, S.A. and M.C. Cabot, *Ceramide-orchestrated signalling in cancer cells.* Nat Rev Cancer, 2013. **13**(1): p. 51-65.
113. Blachnio-Zabielska, A., et al., *Effect of exercise duration on the key pathways of ceramide metabolism in rat skeletal muscles.* J Cell Biochem, 2008. **105**(3): p. 776-84.
114. Lee, S., et al., *Quantitative analysis of sphingomyelin by high-performance liquid chromatography after enzymatic hydrolysis.* Evid Based Complement Alternat Med, 2012. **2012**: p. 396218.
115. Kjellberg, M.A. and P. Mattjus, *Glycolipid transfer protein expression is affected by glycosphingolipid synthesis.* PLoS One, 2013. **8**(7): p. e70283.
116. Sultan, I., et al., *Regulation of the sphingosine-recycling pathway for ceramide generation by oxidative stress, and its role in controlling c-Myc/Max function.* Biochem J, 2006. **393**(Pt 2): p. 513-21.
117. Kitatani, K., et al., *Involvement of acid beta-glucosidase 1 in the salvage pathway of ceramide formation.* J Biol Chem, 2009. **284**(19): p. 12972-8.
118. Hagen, N., et al., *Sphingosine-1-phosphate links glycosphingolipid metabolism to neurodegeneration via a calpain-mediated mechanism.* Cell Death Differ, 2011. **18**(8): p. 1356-65.
119. Le Stunff, H., et al., *Recycling of sphingosine is regulated by the concerted actions of sphingosine-1-phosphate phosphohydrolase 1 and sphingosine kinase 2.* J Biol Chem, 2007. **282**(47): p. 34372-80.
120. Spassieva, S.D., et al., *Cell density-dependent reduction of dihydroceramide desaturase activity in neuroblastoma cells.* J Lipid Res, 2012. **53**(5): p. 918-28.
121. Schumacher, F., et al., *The sphingosine 1-phosphate breakdown product, (2E)-hexadecenal, forms protein adducts and glutathione conjugates in vitro.* J Lipid Res, 2017. **58**(8): p. 1648-1660.
122. Drews, K., et al., *Glucosylceramide synthase maintains influenza virus entry and infection.* PLoS One, 2020. **15**(2): p. e0228735.
123. Dawaliby, R., et al., *Phosphatidylethanolamine Is a Key Regulator of Membrane Fluidity in Eukaryotic Cells.* J Biol Chem, 2016. **291**(7): p. 3658-67.
124. Guo, Q., et al., *Sphingolipids are required for exocyst polarity and exocytic secretion in Saccharomyces cerevisiae.* Cell Biosci, 2020. **10**: p. 53.
125. Guan, X.L., et al., *Functional interactions between sphingolipids and sterols in biological membranes regulating cell physiology.* Mol Biol Cell, 2009. **20**(7): p. 2083-95.
126. Feng, S., et al., *Mitochondria-specific photoactivation to monitor local sphingosine metabolism and function.* Elife, 2018. **7**.
127. Vahey, M.D. and D.A. Fletcher, *Low-Fidelity Assembly of Influenza A Virus Promotes Escape from Host Cells.* Cell, 2019. **176**(1-2): p. 281-294 e19.

128. Xia, C., et al., *Transient inhibition of sphingosine kinases confers protection to influenza A virus infected mice.* Antiviral Res, 2018. **158**: p. 171-177.
129. Vijayan, M. and B. Hahm, *Influenza viral manipulation of sphingolipid metabolism and signaling to modulate host defense system.* Scientifica (Cairo), 2014. **2014**: p. 793815.
130. Tafesse, F.G., et al., *Intact sphingomyelin biosynthetic pathway is essential for intracellular transport of influenza virus glycoproteins.* Proc Natl Acad Sci U S A, 2013. **110**(16): p. 6406-11.
131. Audi, A., et al., *Depletion of Host and Viral Sphingomyelin Impairs Influenza Virus Infection.* Frontiers in Microbiology, 2020. **11**.
132. Senkal, C.E., et al., *Antiapoptotic roles of ceramide-synthase-6-generated C16-ceramide via selective regulation of the ATF6/CHOP arm of ER-stress-response pathways.* FASEB journal : official publication of the Federation of American Societies for Experimental Biology, 2010. **24**(1): p. 296-308.
133. Sassa, T., T. Hirayama, and A. Kihara, *Enzyme Activities of the Ceramide Synthases CERS2-6 Are Regulated by Phosphorylation in the C-terminal Region.* J Biol Chem, 2016. **291**(14): p. 7477-87.
134. Mondal, A., et al., *Influenza virus recruits host protein kinase C to control assembly and activity of its replication machinery.* Elife, 2017. **6**.
135. Breslow, D.K. and J.S. Weissman, *Membranes in balance: mechanisms of sphingolipid homeostasis.* Mol Cell, 2010. **40**(2): p. 267-79.
136. Hannun, Y.A. and L.M. Obeid, *Principles of bioactive lipid signalling: lessons from sphingolipids.* Nat Rev Mol Cell Biol, 2008. **9**(2): p. 139-50.
137. Gault, C.R., L.M. Obeid, and Y.A. Hannun, *An overview of sphingolipid metabolism: from synthesis to breakdown.* Advances in experimental medicine and biology, 2010. **688**: p. 1-23.
138. Osawa, Y., et al., *Roles for C16-ceramide and sphingosine 1-phosphate in regulating hepatocyte apoptosis in response to tumor necrosis factor-alpha.* J Biol Chem, 2005. **280**(30): p. 27879-87.
139. Grafen, A., et al., *Use of Acid Ceramidase and Sphingosine Kinase Inhibitors as Antiviral Compounds Against Measles Virus Infection of Lymphocytes in vitro.* Front Cell Dev Biol, 2019. **7**: p. 218.
140. Miller, M.E., et al., *Ebolavirus requires acid sphingomyelinase activity and plasma membrane sphingomyelin for infection.* J Virol, 2012. **86**(14): p. 7473-83.
141. Aizaki, H., et al., *Critical role of virion-associated cholesterol and sphingolipid in hepatitis C virus infection.* J Virol, 2008. **82**(12): p. 5715-24.
142. Pastenkos, G., et al., *Role of Sphingomyelin in Alphaherpesvirus Entry.* J Virol, 2019. **93**(5).
143. Iwabuchi, K., et al., *Properties and functions of lactosylceramide from mouse neutrophils.* Glycobiology, 2015. **25**(6): p. 655-68.
144. Atkin-Smith, G.K., et al., *The induction and consequences of Influenza A virus-induced cell death.* Cell Death Dis, 2018. **9**(10): p. 1002.
145. Martin, S.F., N. Williams, and S. Chatterjee, *Lactosylceramide is required in apoptosis induced by N-Smase.* Glycoconj J, 2006. **23**(3-4): p. 147-57.

146. Guo, L., et al., *Roles of sphingosine-1-phosphate in reproduction.* Reprod Sci, 2014. **21**(5): p. 550-4.
147. Park, W.J. and J.W. Park, *The effect of altered sphingolipid acyl chain length on various disease models.* Biol Chem, 2015. **396**(6-7): p. 693-705.
148. Aktepe, T.E., H. Pham, and J.M. Mackenzie, *Differential utilisation of ceramide during replication of the flaviviruses West Nile and dengue virus.* Virology, 2015. **484**: p. 241-50.
149. Tatematsu, K., et al., *Host sphingolipid biosynthesis is a promising therapeutic target for the inhibition of hepatitis B virus replication.* J Med Virol, 2011. **83**(4): p. 587-93.